

Introduction to QCD in hadronic collisions

M.L. Mangano

CERN, Geneva, Switzerland

Abstract

I review in this series of lectures the basics of perturbative quantum chromodynamics and some simple applications to the physics of high-energy hadronic collisions.

1 Introduction

Quantum chromodynamics (QCD) is the theory of strong interactions. It is formulated in terms of elementary fields (quarks and gluons), whose interactions obey the principles of a relativistic quantum field theory, with a non-Abelian gauge invariance $SU(3)$. The emergence of QCD as a theory of strong interactions could be reviewed historically, analysing the various experimental data and the theoretical ideas available in the years 1960–1973 (see, for example, Refs. [17, 18]). To do this accurately and usefully would require more time than I have available. I therefore prefer to introduce QCD right away, and to use my time in exploring some of its consequences and applications. I will therefore assume that you all know more or less what QCD is! I assume you know that hadrons are made of quarks, that quarks are spin-1/2, colour-triplet fermions, interacting via the exchange of an octet of spin-1 gluons. I assume you know the concept of running couplings, asymptotic freedom and of confinement. I shall finally assume that you have some familiarity with the fundamental ideas and formalism of quantum electrodynamics (QED): Feynman rules, renormalization, gauge invariance.

If you go through lecture series on QCD (e.g., the lectures given in previous years at the European Schools of High-Energy Physics, Refs. [9–11]), you will hardly ever find the same item twice. This is because QCD today covers a huge set of subjects and each of us has his own concept of what to do with QCD and of what are the ‘fundamental’ notions of QCD and its ‘fundamental’ applications. As a result, you will find lecture series centred around non-perturbative applications, (lattice QCD, sum rules, chiral perturbation theory, heavy-quark effective theory), around formal properties of the perturbative expansion (asymptotic behaviour, renormalons), techniques to evaluate complex classes of Feynman diagrams, or phenomenological applications of QCD to possibly very different sets of experimental data: structure functions, deep-inelastic scattering (DIS) sum rules, polarized DIS, small- x physics (including hard pomerons, diffraction), LEP physics, $p\bar{p}$ collisions, etc.

I will not be able to cover or even to mention all of this. After introducing some basic material, I will focus on some elementary applications of QCD in high-energy phenomena, and in particular on the case of hadron–hadron collisions. The material covered in these lectures includes the following.

1. Gauge invariance and Feynman rules for QCD.
2. The structure of the proton.
3. The evolution of final states: from quarks and gluons to hadrons.
4. Some key hard processes in hadron–hadron collisions: formalism, W/Z production, jet production.

The treatment will be very elementary, and the emphasis will be on basic and intuitive physics concepts. Explicit details and the derivation of equations and formulas is left for a few appendices, covering

- a. renormalization, running coupling, renormalization group invariance;
- b. deep-inelastic scattering and evolution equations;
- c. jet observables in e^+e^- collisions.

Given the large number of papers which have contributed to the development of the field, it is impossible to provide a fair bibliography. I therefore limit my list of references to some excellent books and review articles covering the material presented here, and more. Papers on specific items can be easily found by consulting the standard hep-th and hep-ph preprint archives.

2 QCD Feynman rules

Before starting with the applications, we need to spend some time developing the formalism and the necessary theoretical ideas. I will start from the Feynman rules. I will use an approach which is not canonical, namely it does not follow the standard path of the construction of a gauge-invariant Lagrangian and the derivation of Feynman rules from it. I will rather start from QED, and empirically construct the extension to a non-Abelian theory by enforcing the desired symmetries directly on some specific scattering amplitudes. Hopefully, this will lead to a better insight into the relation between gauge invariance and Feynman rules. It will also provide you with a way of easily recalling or checking your rules when books are not around!

2.1 Summary of QED Feynman rules

We start by summarizing the familiar Feynman rules for QED. They are obtained from the Lagrangian

$$\mathcal{L} = \bar{\psi}(i\cancel{\partial} - m)\psi - e\bar{\psi}A\psi - \frac{1}{4}F_{\mu\nu}F^{\mu\nu} \quad (1)$$

where ψ is the electron field, of mass m and coupling constant e , and $F^{\mu\nu}$ is the electromagnetic field strength.

$$F_{\mu\nu} = \partial_\mu A_\nu - \partial_\nu A_\mu. \quad (2)$$

The resulting Feynman rules are summarized in the following table:

$$\begin{array}{c} \text{p} \\ \longrightarrow \\ \hline \end{array} = \frac{i}{\cancel{p} - m + i\epsilon} = i \frac{\cancel{p} + m}{p^2 - m^2 + i\epsilon} \quad (3)$$

$$\begin{array}{c} \mu \\ \text{p} \\ \text{wavy line} \\ \nu \end{array} = -i \frac{g_{\mu\nu}}{p^2 + i\epsilon} \text{ (Feynman gauge)} \quad (4)$$

$$\begin{array}{c} \text{wavy line} \\ \mu \\ \text{vertex} \end{array} = -ie\gamma_\mu Q \quad (Q = -1 \text{ for the electron, } Q = 2/3 \text{ for the } u\text{-quark, etc.}) \quad (5)$$

Let us start by considering a simple QED process, $e^+e^- \rightarrow \gamma\gamma$ (for simplicity we shall always assume $m = 0$):

$$\begin{array}{c} \text{q} \\ \longrightarrow \\ \text{q} \\ \longleftarrow \end{array} \begin{array}{c} \text{wavy line } k_1, \mu \\ \text{wavy line } k_2, \nu \end{array} \quad \begin{array}{c} \text{q} \\ \longrightarrow \\ \text{q} \\ \longleftarrow \end{array} \begin{array}{c} \text{wavy line } k_1, \mu \\ \text{wavy line } k_2, \nu \end{array} = D_1 + D_2. \quad (6)$$

The total amplitude M_γ is given by

$$\frac{i}{e^2} M_\gamma \equiv D_1 + D_2 = \bar{v}(\bar{q}) \not{\epsilon}_2 \frac{1}{\cancel{q} - \cancel{k}_1} \not{\epsilon}_1 u(q) + \bar{v}(\bar{q}) \not{\epsilon}_1 \frac{1}{\cancel{q} - \cancel{k}_2} \not{\epsilon}_2 n(q) \equiv M_{\mu\nu} \epsilon_1^\mu \epsilon_2^\nu. \quad (7)$$

Gauge invariance demands that

$$\epsilon_2^\nu \partial^\mu M_{\mu\nu} = \epsilon_1^\mu \partial^\nu M_{\mu\nu} = 0. \quad (8)$$

$M_\mu \equiv M_{\mu\nu}\epsilon'_2$ is in fact the current that couples to the photon k_1 . Charge conservation requires $\partial_\mu M^\mu = 0$:

$$\begin{aligned} \partial_\mu M^\mu = 0 &\Rightarrow \frac{d}{dt} \int M^0 d^3x = \int \partial_0 M^0 d^3x \\ &= \int \vec{\nabla} \cdot \vec{M} d^3x = \int_{S \rightarrow \infty} \vec{M} \cdot d\vec{\Sigma} = 0. \end{aligned} \quad (9)$$

In momentum space, this means

$$k_1^\mu M_\mu = 0. \quad (10)$$

Another way of saying this is that the theory is invariant if $\epsilon_\mu(k) \rightarrow \epsilon_\mu(k) + f(k) k_\mu$. This is the standard Abelian gauge invariance associated with the vector potential transformations:

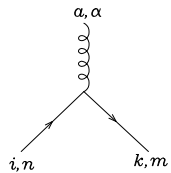
$$A_\mu(x) \rightarrow A_\mu(x) + \partial_\mu f(x). \quad (11)$$

Let us verify that M_γ is indeed gauge invariant. Using $\not{q}u(q) = \bar{v}(\bar{q})\not{\bar{q}} = 0$ from the Dirac equation, we can rewrite $k_1^\mu M_\mu$ as

$$\begin{aligned} k_1^\mu \epsilon'_2 M_{\mu\nu} &= \bar{v}(\bar{q})\not{\epsilon}_2 \frac{1}{\not{q} - \not{k}_1} (\not{k}_1 - \not{q})u(q) + \bar{v}(\bar{q})(\not{k}_1 - \not{\bar{q}}) \frac{1}{\not{k}_1 - \not{\bar{q}}}\not{\epsilon}_2 u(q) \\ &= -\bar{v}(\bar{q})\not{\epsilon}_2 u(q) + \bar{v}(\bar{q})\not{\epsilon}_2 u(q) = 0. \end{aligned} \quad (12)$$

Notice that the two diagrams are not individually gauge invariant, only the sum is. Notice also that the cancellation takes place independently of the choice of ϵ_2 . The amplitude is therefore gauge invariant even in the case of emission of non-transverse photons.

Let us try now to generalize our QED example to a theory where the ‘electrons’ carry a non-Abelian charge, i.e., they transform under a non-trivial representation R of a non-Abelian group G (which, for the sake of simplicity, we shall always assume to be of the $SU(N)$ type. Likewise, we shall refer to the non-Abelian charge as ‘colour’). The standard current operator belongs to the product $R \otimes \bar{R}$. The only representation that belongs to $R \otimes \bar{R}$ for any R is the adjoint representation. Therefore the field that couples to the colour current must transform as the adjoint representation of the group G . So the only generalization of the photon field to the case of a non-Abelian symmetry is a set of vector fields transforming under the adjoint of G , and the simplest generalization of the coupling to fermions takes the form



$$= ig \lambda_{ki}^a \gamma_{mn}^\mu \quad (13)$$

where the matrices λ^a represent the algebra of the group on the representation R . By definition, they satisfy the algebra

$$[\lambda^a, \lambda^b] = if^{abc} \lambda^c \quad (14)$$

for a fixed set of structure constants f^{abc} , which uniquely characterize the algebra. We shall call quarks (q) the fermion fields in R and gluons (g) the vector fields which couple to the quark colour current.

The non-Abelian generalization of the $e^+e^- \rightarrow \gamma\gamma$ process is the $q\bar{q} \rightarrow gg$ annihilation. Its amplitude can be evaluated by including the λ matrices in Eq. (6):

$$\frac{i}{e^2} M_\gamma \rightarrow \frac{i}{g^2} M_g \equiv (\lambda^b \lambda^a)_{ij} D_1 + (\lambda^a \lambda^b)_{ij} D_2 \quad (15)$$

where (a, b) are colour labels (i.e., group indices) of gluons 1 and 2, and (i, j) are colour labels of \bar{q}, q , respectively. Using Eq. (14), we can rewrite Eq. (15) as

$$M_g = (\lambda^a \lambda^b)_{ij} M_\gamma - g^2 f^{abc} \lambda_{ij}^c D_1. \quad (16)$$

If we want the charge associated with the group G to be conserved, we still need to demand

$$k_1^\mu \epsilon_2^\nu M_g^{\mu\nu} = \epsilon_1^\mu k_2^\nu M_g^{\mu\nu} = 0. \quad (17)$$

Substituting $\epsilon_1^\mu \rightarrow k_1^\mu$ in Eq. (16) we get instead, using Eq. (12),

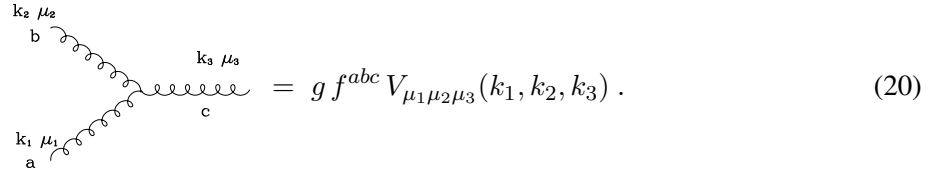
$$k_{1\mu} M_g^\mu = -g^2 f^{abc} \lambda_{ij}^c \bar{v}_i(\bar{q}) \not{\epsilon}_2 u_i(q). \quad (18)$$

The gauge cancellation taking place in QED between the two diagrams is spoiled by the non-Abelian nature of the coupling of quarks to gluons (i.e., λ^a and λ^b do not commute, and $f^{abc} \neq 0$).

The only possible way to solve this problem is to include additional diagrams. That new interactions should exist is by itself a reasonable fact, since gluons are charged (i.e., they transform under the symmetry group) and might want to interact among themselves. If we rewrite Eq. (18) as

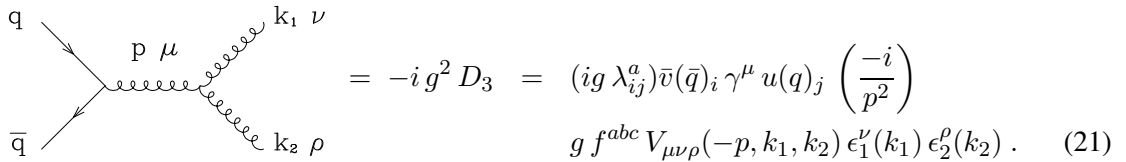
$$k_{1\mu} M_g^\mu = i \left(f^{abc} g \epsilon_2^\mu \right) \times \left(i g \lambda_{ij}^c \bar{v}(\bar{q}) \gamma_\mu u(q) \right), \quad (19)$$

we can recognize in the second factor the structure of the $q\bar{q}g$ vertex. The first factor has the appropriate colour structure to describe a triple-gluon vertex, with a, b, c the colour labels of the three gluons:



$$= g f^{abc} V_{\mu_1 \mu_2 \mu_3}(k_1, k_2, k_3). \quad (20)$$

Equation (19) therefore suggests the existence of a coupling like Eq. (20), with a Lorentz structure $V_{\mu_1 \mu_2 \mu_3}$ to be specified, giving rise to the following contribution to $q\bar{q} \rightarrow gg$:



$$= -i g^2 D_3 = (i g \lambda_{ij}^a) \bar{v}(\bar{q})_i \gamma^\mu u(q)_j \left(\frac{-i}{p^2} \right) g f^{abc} V_{\mu\nu\rho}(-p, k_1, k_2) \epsilon_1^\nu(k_1) \epsilon_2^\rho(k_2). \quad (21)$$

We now need to find $V_{\mu_1 \mu_2 \mu_3}(p_1, p_2, p_3)$ and to verify that the contribution of the new diagram to $k_1 \cdot M_g$ cancels that of the first two diagrams. We will now show that the constraints of Lorentz invariance, Bose symmetry and dimensional analysis uniquely fix V , up to an overall constant factor.

Dimensional analysis fixes the coupling to be linear in the gluon momenta. This is because each vector field carries dimension 1, there are three of them, and the interaction must have total dimension equal to 4. So at most one derivative (i.e., one power of momentum) can appear at the vertex. In principle, if some mass parameter were available, higher derivatives could be included, with the appropriate powers of the mass parameter appearing in the denominator. This is however not the case. It is important to remark that the absence of interactions with a higher number of derivatives is also crucial for the renormalizability of the interaction.

Lorentz invariance requires then that V be built out of terms of the form $g_{\mu_1 \mu_2} p_{\mu_3}$. Bose symmetry requires V to be fully antisymmetric under the exchange of any pair $(\mu_i, p_i) \leftrightarrow (\mu_j, p_j)$ since the colour structure f^{abc} is totally antisymmetric. As a result, for example, a term like $g_{\mu_1 \mu_2} p_3^{\mu_3}$ vanishes under

antisymmetrization, while $g_{\mu_1\mu_2}p_1^{\mu_3}$ does not. Starting from this last term, we can easily add the pieces required to obtain the full antisymmetry in all three indices. The result is unique, up to an overall factor:

$$V_{\mu_1\mu_2\mu_3} = V_0 [(k_1 - k_2)^{\mu_3} g_{\mu_1\mu_2} + (k_2 - k_3)^{\mu_1} g_{\mu_2\mu_3} + (k_3 - k_1)^{\mu_2} g_{\mu_1\mu_3}] . \quad (22)$$

To test the gauge variation of the contribution D_3 , we set $\mu_3 = \mu$, $\epsilon_1 = k_1$ and $k_3 = -(k_1 + k_2)$ in Eq. (21), and we get

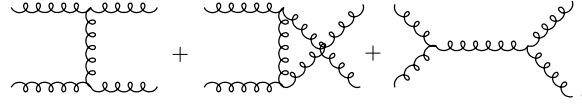
$$k_1^{\mu_1} \epsilon_2^{\mu_2} V_{\mu_1\mu_2\mu} (k_1, k_2, k_3) = V_0 \{ -(k_1 + k_2)^\mu (k_1 \cdot \epsilon_2) + 2(k_1 \cdot k_2) \epsilon_2^\mu - (k_2 \cdot \epsilon_2) k_1^\mu \} . \quad (23)$$

The gauge variation is therefore

$$k_1 \cdot D_3 = g^2 f^{abc} \lambda^c V_0 \left[\bar{v}(\bar{q}) \not{\epsilon}_2 u(q) - \frac{k_2 \cdot \epsilon_2}{2k_1 k_2} \bar{v}(\bar{q}) \not{k}_1 u(q) \right] . \quad (24)$$

The first term cancels the gauge variation of $D_1 + D_2$ provided $V_0 = 1$; the second term vanishes for a physical gluon k_2 , since in this case $k_2 \cdot \epsilon_2 = 0$. $D_1 + D_2 + D_3$ is therefore gauge invariant but, contrary to the case of QED, only for physical external on-shell gluons.

Having introduced a three-gluon coupling, we can induce processes involving only gluons, such as $gg \rightarrow gg$:



$$\quad (25)$$

Once more it is necessary to verify the gauge invariance of this amplitude. It turns out that one more diagram is required, induced by a four-gluon vertex. Lorentz invariance, Bose symmetry and dimensional analysis uniquely determine once again the structure of this vertex. The overall factor is fixed by gauge invariance. The resulting Feynman rule for the four-gluon vertex is given in Fig. 1.

You can verify that the three- and four-gluon vertices we introduced above are exactly those which arise from the Yang–Mills Lagrangian:

$$\mathcal{L}_{\text{YM}} = -\frac{1}{4} \sum_a F_{\mu\nu}^a F^{a\mu\nu} \quad \text{with} \quad F_{\mu\nu}^a = \partial_{[\mu} A_{\nu]}^a - g f^{abc} A_{[\mu}^b A_{\nu]}^c . \quad (26)$$

It can be shown that the three- and four-gluon vertices we generated are all is needed to guarantee gauge invariance even for processes more complicated than those studied in the previous simple examples. In other words, no extra five-or-more-gluon vertices have to be introduced to achieve the gauge invariance of higher-order amplitudes. At the tree level this is the consequence of dimensional analysis and of the locality of the couplings (no inverse powers of the momenta can appear in the Lagrangian). At the loop level, these conditions are supplemented by the renormalizability of the theory [3, 7].

Before one can start calculating cross-sections, a technical subtlety that arises in QCD when squaring the amplitudes and summing over the polarization of external states needs to be discussed. Let us again start from the QED example. Let us focus, for example, on the sum over polarizations of photon k_1 :

$$\sum_{\epsilon_1} |M|^2 = \left(\sum_{\epsilon_1} \epsilon_1^\mu \epsilon_1^{\nu*} \right) M_\mu M_\nu^* . \quad (27)$$

The two independent physical polarizations of a photon with momentum $k = (k_0; 0, 0, k_0)$ are given by $\epsilon_{L,R}^\mu = (0; 1, \pm i, 0)/\sqrt{2}$. They satisfy the standard normalization properties:

$$\epsilon_L \cdot \epsilon_L^* = -1 = \epsilon_R \cdot \epsilon_R^* \quad \epsilon_L \cdot \epsilon_R^* = 0$$

$$\begin{aligned}
 & a, \alpha \text{ --- } \overset{p}{\text{~~~~~}} \text{ --- } b, \beta &= \delta^{ab} \frac{-i g^{\alpha\beta}}{p^2 + i\epsilon} \quad (\text{Feynman gauge}) \\
 & a \text{ --- } \overset{p}{\text{-----}} \text{ --- } b &= \delta^{ab} \frac{i}{p^2 + i\epsilon} \\
 & i, n \text{ --- } \overset{p}{\text{-----}} \text{ --- } k, m &= \delta^{ik} \frac{i}{\not{p} - m + i\epsilon} \Big|_{mn} \\
 \\
 & \begin{array}{c} b, \beta \\ | \\ \text{~~~~~} \\ / \quad \backslash \\ \overset{p}{\text{~~~~~}} \quad \overset{r}{\text{~~~~~}} \\ | \quad | \\ a, \alpha \quad c, \gamma \\ \backslash \quad / \\ \text{~~~~~} \\ / \quad \backslash \\ \overset{p}{\text{~~~~~}} \quad \overset{r}{\text{~~~~~}} \\ | \quad | \\ a, \alpha \quad b, \beta \\ \backslash \quad / \\ \text{~~~~~} \\ / \quad \backslash \\ \overset{p}{\text{~~~~~}} \quad \overset{r}{\text{~~~~~}} \\ | \quad | \\ c, \gamma \quad d, \delta \end{array} &= g f^{abc} \left[g^{\alpha\beta} (p - q)^\gamma + g^{\beta\gamma} (q - r)^\alpha + g^{\gamma\alpha} (r - p)^\beta \right] \\
 \\
 & \begin{array}{c} a, \alpha \\ | \\ \text{~~~~~} \\ / \quad \backslash \\ \text{-----} \quad \text{-----} \\ | \quad | \\ b \quad c \\ \backslash \quad / \\ \text{~~~~~} \\ / \quad \backslash \\ \text{-----} \quad \text{-----} \\ | \quad | \\ a, \alpha \\ \backslash \quad / \\ \text{~~~~~} \\ / \quad \backslash \\ \text{-----} \quad \text{-----} \\ | \quad | \\ c, \gamma \quad d, \delta \end{array} &= -i g^2 f^{xac} f^{xbd} \left(g^{\alpha\beta} g^{\gamma\delta} - g^{\alpha\delta} g^{\beta\gamma} \right) \\
 & & -i g^2 f^{xad} f^{xbc} \left(g^{\alpha\beta} g^{\gamma\delta} - g^{\alpha\gamma} g^{\beta\delta} \right) \\
 & & -i g^2 f^{xab} f^{xcd} \left(g^{\alpha\gamma} g^{\beta\delta} - g^{\alpha\delta} g^{\beta\gamma} \right) \\
 \\
 & \begin{array}{c} a, \alpha \\ | \\ \text{~~~~~} \\ / \quad \backslash \\ \text{-----} \quad \text{-----} \\ | \quad | \\ b \quad c \\ \backslash \quad / \\ \text{~~~~~} \\ / \quad \backslash \\ \text{-----} \quad \text{-----} \\ | \quad | \\ a, \alpha \\ \backslash \quad / \\ \text{~~~~~} \\ / \quad \backslash \\ \text{-----} \quad \text{-----} \\ | \quad | \\ i, n \quad k, m \end{array} &= -g f^{abc} q^\alpha \\
 \\
 & \begin{array}{c} a, \alpha \\ | \\ \text{~~~~~} \\ / \quad \backslash \\ \text{-----} \quad \text{-----} \\ | \quad | \\ b \quad c \\ \backslash \quad / \\ \text{~~~~~} \\ / \quad \backslash \\ \text{-----} \quad \text{-----} \\ | \quad | \\ a, \alpha \\ \backslash \quad / \\ \text{~~~~~} \\ / \quad \backslash \\ \text{-----} \quad \text{-----} \\ | \quad | \\ i, n \quad k, m \end{array} &= i g \lambda_{ki}^a \gamma_{mn}^\alpha
 \end{aligned}$$

Fig. 1: Feynman rules for QCD. The solid lines represent the fermions, the curly lines the gluons, and the dotted lines the ghosts.

We can write the sum over physical polarizations in a convenient form by introducing the vector $\bar{k} = (k_0; 0, 0, -k_0)$:

$$\sum_{i=L,R} \epsilon_i^\mu \epsilon_i^{\nu*} \equiv \begin{pmatrix} 0 & \vec{0} \\ \vec{0} & \begin{matrix} 1 & 0 & 0 \\ 0 & 1 & 0 \\ 0 & 0 & 0 \end{matrix} \end{pmatrix} = -g_{\mu\nu} + \frac{k_\mu \bar{k}_\nu + k_\nu \bar{k}_\mu}{k \cdot \bar{k}}. \quad (28)$$

We could have written the sum over physical polarizations using any other momentum ℓ_μ , provided $k \cdot \ell \neq 0$. This would be equivalent to a gauge transformation (prove it as an exercise). In QED the second term in Eq. (28) can be safely dropped, since $k_\mu M^\mu = 0$. As a cross-check, notice that $k_\mu M^\mu = 0$ implies $M_0 = M_3$, and therefore

$$\sum_{i=L,R} |\epsilon_i \cdot M|^2 = |M_1|^2 + |M_2|^2 = |M_1|^2 + |M_2|^2 + |M_3|^2 - |M_0|^2 \equiv -g^{\mu\nu} M_\mu M_\nu^*. \quad (29)$$

Therefore, the production of the longitudinal and time-like components of the photon cancel each other. This is true *regardless* of whether additional external photons are physical or not, since the gauge invariance $k_1 \cdot M = 0$ shown in Eq. (12) holds regardless of the choice for ϵ_2 , as already remarked. In particular,

$$k_1^{\mu_1} k_2^{\mu_2} M_{\mu_1 \mu_2} = 0 \quad (30)$$

(for n photons, $k_1^{\mu_1} k_2^{\mu_2} \dots k_n^{\mu_n} M_{\mu_1 \dots \mu_n} = 0$) and the production of *any* number of unphysical photons vanishes. The situation in the case of gluon emission is different, since $k_1 \cdot M \propto \epsilon_2 \cdot k_2$, which vanishes only for a physical ϵ_2 . This implies that the production of one physical gluon and one non-physical gluon is equal to 0, but the production of a pair of non-physical gluons is allowed! If $\epsilon_2 \cdot k_2 \neq 0$, then M_0 is not equal to M_3 , and Eq. (28) is not equivalent to $\sum \epsilon_\mu \epsilon_\nu^* = -g_{\mu\nu}$.

Exercise: show that

$$\sum_{\text{non-physical}} |\epsilon_1^\mu \epsilon_2^\nu M_{\mu\nu}|^2 = \left| i g^2 f^{abc} \lambda^c \frac{1}{2k_1 k_2} \bar{v}(\bar{q}) \not{k}_1 u(q) \right|^2. \quad (31)$$

In the case of non-Abelian theories, it is therefore important to restrict the sum over polarizations and (because of unitarity) the off-shell propagators to physical degrees of freedom with the choice of physical gauges. Alternatively, one has to undertake a study of the implications of gauge-fixing in non-physical gauges for the quantization of the theory (see Refs. [3, 7]). The outcome of this analysis is the appearance of two colour-octet scalar degrees of freedom (called ghosts) whose rôle is to enforce unitarity in non-physical gauges. They will appear in internal closed loops, or will be pair-produced in final states. They only couple to gluons. Their Feynman rules are supplemented by the prescription that each closed loop should come with a -1 sign, as if they obeyed Fermi statistics. Being scalars, this prescription breaks the spin-statistics relation, and leads as a result to the possibility that production probabilities are negative. This is precisely what is required to cancel the contributions of non-transverse degrees of freedom appearing in non-physical gauges. Adding the ghosts contribution to $q\bar{q} \rightarrow g\bar{g}$ decays (using the Feynman rules from Fig. 1) gives in fact

$$\left| \begin{array}{c} \text{---} \nearrow \\ \text{---} \searrow \\ \text{---} \text{---} \text{---} \\ \text{---} \nearrow \\ \text{---} \searrow \end{array} \right|^2 = - \left| i g^2 f^{abc} \lambda^c \frac{1}{2k_1 k_2} \bar{v}(\bar{q}) \not{k}_1 u(q) \right|^2, \quad (32)$$

which exactly cancels the contribution of non-transverse gluons in the non-physical gauge $\sum \epsilon_\mu \epsilon_\nu^* = -g_{\mu\nu}$, given in in Eq. (31).

$$\frac{1}{\sqrt{2}} \left(\begin{array}{c} \text{---} \uparrow \downarrow \text{---} \\ \text{---} \uparrow \downarrow \text{---} \\ \text{---} \uparrow \downarrow \text{---} \end{array} - \frac{1}{N} \begin{array}{c} \text{---} \uparrow \downarrow \text{---} \\ \text{---} \uparrow \downarrow \text{---} \\ \text{---} \uparrow \downarrow \text{---} \end{array} \right) \quad \text{fermion-gluon vertex } (t^a) \quad (40)$$

$$\frac{1}{\sqrt{2}} \left(\begin{array}{c} \text{---} \uparrow \downarrow \text{---} \\ \text{---} \uparrow \downarrow \text{---} \\ \text{---} \uparrow \downarrow \text{---} \end{array} - \begin{array}{c} \text{---} \uparrow \downarrow \text{---} \\ \text{---} \uparrow \downarrow \text{---} \\ \text{---} \uparrow \downarrow \text{---} \end{array} \right) \quad \text{3-gluon vertex } (f^{abc}). \quad (41)$$

Contraction over colour indices is obtained by connecting the respective colour (or anticolour) lines. A closed loop of a colour line gives rise to a factor N , since the closed loop is equivalent to the trace of the unit matrix. So the above representation of the $q\bar{q}g$ vertex embodies the idea of ‘colour conservation’, whereby the colour-anticolour quantum numbers carried by the $q\bar{q}$ pair are transferred to the gluon. The piece proportional to $1/N$ in the $q\bar{q}g$ vertex appears only when the colour of the quark and of the antiquark are the same. It ensures that λ^a is traceless, as it should be. This can be easily checked as an exercise. The factor $1/\sqrt{2}$ is related to the chosen normalization of T_F .

As a first example of applications, let us re-evaluate C_F :

$$\begin{aligned} i \xrightarrow{\lambda^a} \text{---} \uparrow \downarrow \text{---} \xrightarrow{\lambda^a} j &= \frac{1}{\sqrt{2}} \left(\begin{array}{c} \text{---} \uparrow \downarrow \text{---} \\ \text{---} \uparrow \downarrow \text{---} \\ \text{---} \uparrow \downarrow \text{---} \end{array} - \frac{1}{N} \begin{array}{c} \text{---} \uparrow \downarrow \text{---} \\ \text{---} \uparrow \downarrow \text{---} \\ \text{---} \uparrow \downarrow \text{---} \end{array} \right) \times \frac{1}{\sqrt{2}} \left(\begin{array}{c} \text{---} \uparrow \downarrow \text{---} \\ \text{---} \uparrow \downarrow \text{---} \\ \text{---} \uparrow \downarrow \text{---} \end{array} - \frac{1}{N} \begin{array}{c} \text{---} \uparrow \downarrow \text{---} \\ \text{---} \uparrow \downarrow \text{---} \\ \text{---} \uparrow \downarrow \text{---} \end{array} \right) \\ &= \frac{1}{2} \left(\begin{array}{c} \text{---} \uparrow \downarrow \text{---} \\ \text{---} \uparrow \downarrow \text{---} \\ \text{---} \uparrow \downarrow \text{---} \end{array} \xrightarrow{N} \begin{array}{c} \text{---} \uparrow \downarrow \text{---} \\ \text{---} \uparrow \downarrow \text{---} \\ \text{---} \uparrow \downarrow \text{---} \end{array} - \frac{1}{N} \begin{array}{c} \text{---} \uparrow \downarrow \text{---} \\ \text{---} \uparrow \downarrow \text{---} \\ \text{---} \uparrow \downarrow \text{---} \end{array} \xrightarrow{N} \begin{array}{c} \text{---} \uparrow \downarrow \text{---} \\ \text{---} \uparrow \downarrow \text{---} \\ \text{---} \uparrow \downarrow \text{---} \end{array} - \frac{1}{N} \begin{array}{c} \text{---} \uparrow \downarrow \text{---} \\ \text{---} \uparrow \downarrow \text{---} \\ \text{---} \uparrow \downarrow \text{---} \end{array} \xrightarrow{N} \begin{array}{c} \text{---} \uparrow \downarrow \text{---} \\ \text{---} \uparrow \downarrow \text{---} \\ \text{---} \uparrow \downarrow \text{---} \end{array} + \\ &\quad + \frac{1}{N^2} \begin{array}{c} \text{---} \uparrow \downarrow \text{---} \\ \text{---} \uparrow \downarrow \text{---} \\ \text{---} \uparrow \downarrow \text{---} \end{array} \xrightarrow{N} \begin{array}{c} \text{---} \uparrow \downarrow \text{---} \\ \text{---} \uparrow \downarrow \text{---} \\ \text{---} \uparrow \downarrow \text{---} \end{array} \Big) = \delta^{ij} \frac{N^2 - 1}{2N}. \end{aligned} \quad (42)$$

As an exercise, you can calculate the colour factor for $q\bar{q} \rightarrow q\bar{q}$ scattering, and show that

$$\sum_a (\lambda^a)_{ij} (\lambda^a)_{lk} = \begin{array}{c} j \\ \uparrow \\ \text{---} \uparrow \downarrow \text{---} \\ \downarrow \\ k \\ i \end{array} = \frac{1}{2} \left(\begin{array}{c} \uparrow \downarrow \\ \text{---} \uparrow \downarrow \text{---} \\ \uparrow \downarrow \end{array} - \frac{1}{N} \begin{array}{c} \uparrow \downarrow \\ \text{---} \uparrow \downarrow \text{---} \\ \uparrow \downarrow \end{array} \right) = \frac{1}{2} \left(\delta_{ik} \delta_{lj} - \frac{1}{N} \delta_{ij} \delta_{lk} \right). \quad (43)$$

This result can be used to evaluate the one-loop colour factors for the interaction vertex with a photon:

$$\begin{array}{c} \text{---} \uparrow \downarrow \text{---} \\ \uparrow \downarrow \\ \text{---} \uparrow \downarrow \text{---} \end{array} = \frac{1}{2} \left(\begin{array}{c} \text{---} \uparrow \downarrow \text{---} \\ \uparrow \downarrow \\ \text{---} \uparrow \downarrow \text{---} \end{array} - \frac{1}{N} \begin{array}{c} \text{---} \uparrow \downarrow \text{---} \\ \uparrow \downarrow \\ \text{---} \uparrow \downarrow \text{---} \end{array} \right) = \frac{1}{2} \frac{N^2 - 1}{N} \delta_{ij} = C_F \delta_{ij}. \quad (44)$$

For the interaction with a gluon, we have instead

$$\begin{array}{c} \text{---} \uparrow \downarrow \text{---} \\ \uparrow \downarrow \\ \text{---} \uparrow \downarrow \text{---} \end{array} = \frac{1}{\sqrt{2}} \left(\begin{array}{c} \text{---} \uparrow \downarrow \text{---} \\ \uparrow \downarrow \\ \text{---} \uparrow \downarrow \text{---} \end{array} - \frac{1}{N} \begin{array}{c} \text{---} \uparrow \downarrow \text{---} \\ \uparrow \downarrow \\ \text{---} \uparrow \downarrow \text{---} \end{array} \right) \times \frac{1}{2} \left(\begin{array}{c} \uparrow \downarrow \\ \text{---} \uparrow \downarrow \text{---} \\ \uparrow \downarrow \end{array} - \frac{1}{N} \begin{array}{c} \uparrow \downarrow \\ \text{---} \uparrow \downarrow \text{---} \\ \uparrow \downarrow \end{array} \right)$$

$$\begin{aligned}
&= \frac{1}{2\sqrt{2}} \left(\begin{array}{c} \text{Diagram 1} \\ \text{Diagram 2} \\ \text{Diagram 3} \\ \text{Diagram 4} \end{array} \right) \\
&= -\frac{1}{2N} \frac{1}{\sqrt{2}} \left(\begin{array}{c} \text{Diagram 5} \\ \text{Diagram 6} \end{array} \right) = -\frac{1}{2N} \begin{array}{c} \text{Diagram 7} \end{array} . \quad (45)
\end{aligned}$$

Note that in the case of the coupling to the photon, the $q\bar{q}$ pair is in a colour-singlet state and the gluon exchange effect has a positive sign (\Rightarrow attraction). In the case of the coupling to the gluon, the $q\bar{q}$ pair is in a colour-octet state and the gluon-exchange correction has a negative sign relative to the Born interaction. The force between a $q\bar{q}$ pair is therefore *attractive* if the pair is in a colour-singlet state, and *repulsive* if it is in a colour-octet state! This gives a qualitative argument for why no colour-octet $q\bar{q}$ bound state exists.

The remaining important relation that one needs is the following:

$$\sum_{a,b} f^{abc} f^{abd} = C_A \delta^{cd} \quad \text{with } C_A = N . \quad (46)$$

You can easily prove it by using the graphical representation given in Eq. (41), or by using Eq. (43) and $f^{abc} = -2i \text{tr}([\lambda^a, \lambda^b] \lambda^c)$.

3 QCD and the proton structure at large Q^2

The understanding of the structure of the proton at short distances is one of the key ingredients to be able to predict cross-section for processes involving hadrons in the initial state. All processes in hadronic collisions, even those intrinsically of electroweak nature such as the production of W/Z bosons or photons, are in fact induced by the quarks and gluons contained inside the hadron. In this lecture I will introduce some important concepts, such as the notion of partonic densities of the proton, and of parton evolution. These are the essential tools used by theorists to predict production rates for hadronic reactions.

We shall limit ourselves to processes where a proton-(anti)proton pair collides at high centre-of-mass energy (\sqrt{S} , typically larger than several hundred GeV) and undergoes a strongly inelastic interaction, with momentum transfers between the participants in excess of several GeV. The outcome of this hard interaction could be the simple scattering at large angle of some of the hadron's elementary constituents, their annihilation into new massive resonances, or a combination of the two. In all cases the final state consists of a large multiplicity of particles, associated with the evolution of the fragments of the initial hadrons, as well as of the new states produced. As discussed below, the fundamental physical concept that makes this programme possible is 'factorization', the ability to isolate separate independent phases of the overall collision. These phases are dominated by different dynamics, and the most appropriate techniques can be applied to describe each of them separately. In particular, factorization allows one to decouple the complexity of the proton structure and of the final-state hadron formation from the elementary nature of the perturbative hard interaction among parton constituents.

Figure 2 illustrates how this works. As the left proton travels freely before coming into contact with the hadron coming in from the right, its constituent quarks are held together by the constant exchange of virtual gluons (e.g., gluons a and b in the picture). These gluons are mostly soft, because any hard exchange would cause the constituent quarks to fly apart, and a second hard exchange would be necessary to re-establish the balance of momentum and keep the proton together. Gluons of high virtuality (gluon c in the picture) prefer therefore to be reabsorbed by the same quark, within a time inversely

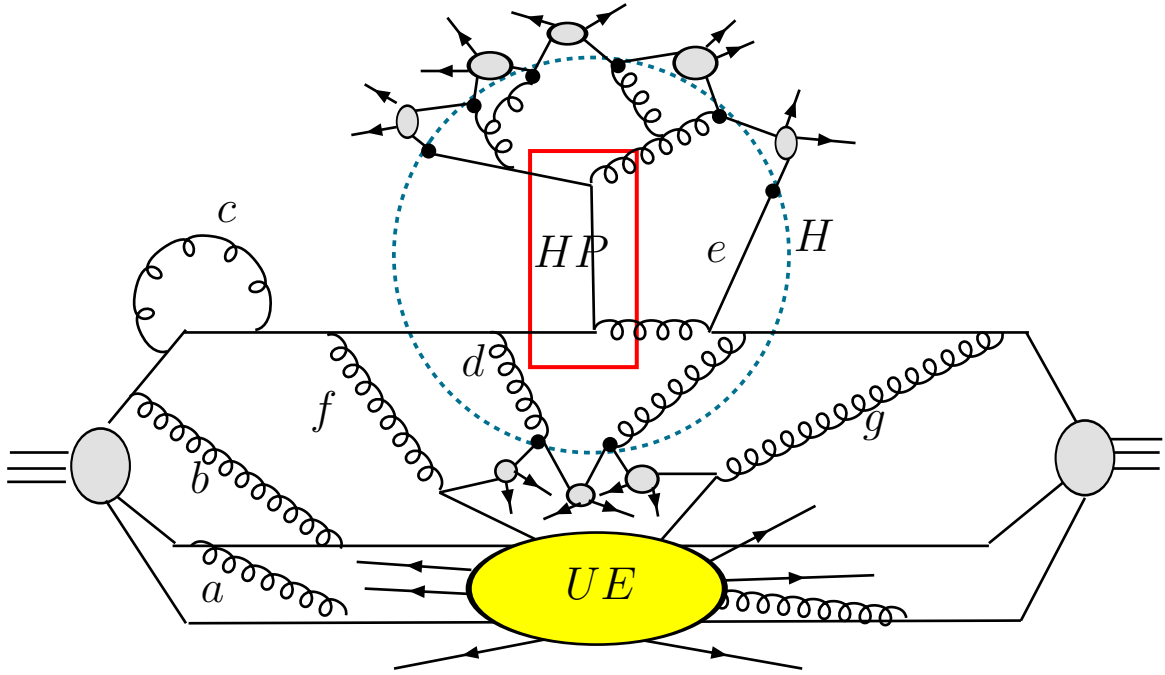


Fig. 2: General structure of a hard proton–proton collision

proportional to their virtuality, as prescribed by the uncertainty principle. The state of the quark is, however, left unchanged by this process. Altogether this suggests that the global state of the proton, although defined by a complex set of gluon exchanges between quarks, is nevertheless determined by interactions which have a time scale of the order of $1/m_p$. When seen in the laboratory frame where the proton is moving with energy $\sqrt{S}/2$, this time is furthermore Lorentz dilated by a factor $\gamma = \sqrt{S}/2m_p$. If we disturb a quark with a probe of virtuality $Q \gg m_p$, the time frame for this interaction is so short ($1/Q$) that the interactions of the quark with the rest of the proton can be neglected. The struck quark cannot negotiate with its partners a coherent response to the external perturbation: it simply does not have the time to communicate to them that it is being kicked away. On this time scale, only gluons with energy of the order of Q can be emitted, something which, to happen coherently over the whole proton, is suppressed by powers of m_p/Q (this suppression characterizes the ‘elastic form factor’ of the proton). In this figure, the hard process is represented by the rectangle labelled HP. In this example a head-on collision with a gluon from the opposite hadron, leads to a $qg \rightarrow qg$ scattering with a momentum exchange of the order of Q . This and other possible processes can be calculated from first principles in perturbative QCD.

When the constituent is suddenly deflected, the partons that it had recently radiated cannot be reabsorbed (as happened to gluon c earlier) because the constituent is no longer there waiting for the partons to come back. This is the case, for example, of the gluon d emitted by the quark, and of the quark e from the opposite hadron; the emitted gluon got engaged in the hard interaction. The number of ‘liberated’ partons will depend on the hard scale Q : the larger Q , the more sudden the deflection of the struck parton, and the fewer the partons that can reconnect before its departure (typically only partons with virtuality larger than Q).

After the hard process, the partons liberated during the evolution prior to the collision and the partons created by the hard collision will themselves emit radiation. The radiation process, governed by perturbative QCD, continues until a low virtuality scale is reached (the boundary region labelled with a dotted line, H, in our figure). To describe this perturbative evolution phase, proper care has to be taken to incorporate quantum coherence effects, which in principle connect the probabilities of radiation off different partons in the event. Once the low virtuality scale is reached the memory of the

hard-process phase has been lost, once again as a result of different time scales in the problem, and the final phase of hadronization takes over. Because of the decoupling from the hard-process phase, the hadronization is assumed to be independent of the initial hard process, and its parametrization, tuned to the observables of some reference process, can then be used in other hard interactions (universality of hadronization). Nearby partons merge into colour-singlet clusters (the grey blobs in Fig. 2), which are then decayed phenomenologically into physical hadrons. To complete the picture, we need to understand the evolution of the fragments of the initial hadrons. As shown in the figure, this evolution cannot be entirely independent of what happens in the hard event, because at least colour quantum numbers must be exchanged to guarantee the overall neutrality and conservation of baryon number. In our example, the gluons f and g , emitted early on in the perturbative evolution of the initial state, split into $q\bar{q}$ pairs which are shared between the hadron fragments (whose overall interaction is represented by the oval labelled UE, for Underlying Event) and the clusters resulting from the evolution of the initial state.

The above ideas are embodied in the following factorization formula, which represents the starting point of any theoretical analysis of cross-sections and observables in hadronic collisions:

$$\frac{d\sigma}{dX} = \sum_{j,k} \int_{\hat{X}} f_j(x_1, Q_i) f_k(x_2, Q_i) \frac{d\hat{\sigma}_{jk}(Q_i, Q_f)}{d\hat{X}} F(\hat{X} \rightarrow X; Q_i, Q_f), \quad (47)$$

where

- X is some hadronic observable (e.g., the transverse momentum of a pion);
- the sum over j and k extends over the parton types inside the colliding hadrons;
- the function $f_j(x, Q)$ (known as parton distribution function, PDF) represents the number density of parton type j with momentum fraction x in a proton probed at a scale Q_i ;
- \hat{X} is a parton-level observable (e.g., the transverse momentum of a parton from the hard scattering);
- $\hat{\sigma}_{jk}$ is the parton-level cross-section, differential in the observable \hat{X} ;
- $F(\hat{X} \rightarrow X; Q_i, Q_f)$ is a transition function, weighting the probability that the partonic state defining \hat{X} gives rise to the hadronic observable X ;
- the scales Q_i and Q_f correspond to the scales at which we separate the perturbative, hard process from the initial- and final-state evolutions, respectively.

In the rest of this section I shall cover the above ideas in some more detail. While I will not provide you with a rigorous proof of the legitimacy of this approach, I will try to justify it qualitatively to make it sound at least plausible. In Appendix B I will collect some more explicit derivations and results.

3.1 The parton densities and their evolution

As mentioned above, the binding forces responsible for the quark confinement are due to the exchange of rather soft gluons. If a quark were to exchange a hard virtual gluon with another quark, in fact, the recoil would tend to break the proton apart. It is easy to verify that the exchange of gluons with virtuality larger than Q is then proportional to some large power of m_p/Q , m_p being the proton mass. Since the gluon coupling constant gets smaller at large Q , exchange of hard gluons is significantly suppressed¹. Consider in fact the picture Fig. 3. The exchange of two gluons is required to ensure that the momentum exchanged after the first gluon emission is returned to the quark, and the proton maintains its structure. The contributions of hard gluons to this process can be approximated by integrating the loop over large momenta:

$$\int_Q \frac{d^4q}{q^6} \sim \frac{1}{Q^2}. \quad (48)$$

¹The fact that the coupling decreases at large Q plays a fundamental role in this argument. Were this not true, the parton picture could not be used!

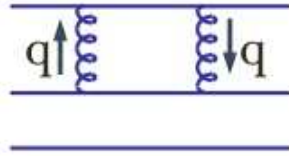


Fig. 3: Gluon exchange inside the proton

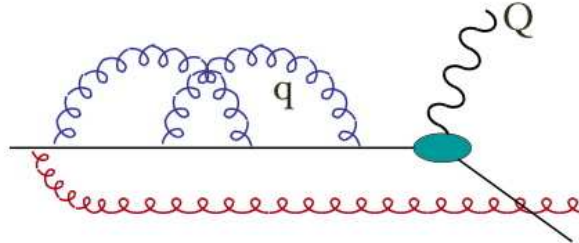


Fig. 4: Gluon emission at different scales during the approach to a hard collision

At large Q this contribution is suppressed by powers of $(m_p/Q)^2$, where the proton mass m_p is included as being the only dimensionful quantity available. The interactions keeping the proton together are therefore dominated by soft exchanges, with virtuality Q of the order of m_p . The typical time scale of these exchanges is of the order of $1/m_p$ (in the laboratory system, where the proton travels with energy E , this time is Lorentz dilated to $\tau \sim \gamma/m_p = E/m_p^2$). If we probe the proton with an off-shell photon, the interaction takes place during the limited lifetime of the virtual photon, given by the inverse of its virtuality as a result of the Heisenberg principle. Assuming the virtuality $Q \gg m_p$, once the photon gets ‘inside’ the proton and meets a quark, the struck quark has no time to negotiate a coherent response with the other quarks, because the time scale for it to ‘talk’ to its pals is too long compared with the duration of the interaction with the photon itself. As a result, the struck quark has no option but to interact with the photon as if it were a free particle.

Let us look in more detail at what happens during such process. In Fig. 4 we see a proton as it approaches a hard collision with a photon of virtuality Q . Gluons emitted at a scale $q > Q$ have the time to be reabsorbed, since their lifetime is very short. Their contribution to the process can be calculated in perturbative QCD, since the scale is large. Since after being reabsorbed the state of the quark remains the same, their only effect is an overall renormalization of the wave function, and they do not affect the quark density. A gluon emitted at a scale $q < Q$, however, has a lifetime longer than the time it takes for the quark to interact with the photon, and by the time it tries to reconnect to its parent quark, the quark has been kicked away by the photon, and is no longer there. Since the gluon has taken away some of the quark momentum, the momentum fraction x of the quark as it enters the interaction with the photon is different from the momentum it had before, and therefore its density $f(x)$ is affected. Furthermore, when the scale q is of the order of 1 GeV the state of the quark is not calculable in perturbative QCD. This state depends on the internal wave function of the proton, which perturbative QCD cannot easily predict. We can however say that the wave function of the proton, and therefore the state of the ‘free’ quark, are determined by the dynamics of the soft-gluon exchanges inside the proton itself. Since the time scale of this dynamics is long relative to the time scale of the photon–quark interaction, we can safely argue that the photon sees to good approximation a static snapshot of the proton’s inner guts. In other words, the state of the quark had been prepared long before the photon arrived. This also suggests that the state of the quark will not depend on the precise nature of the external probe, provided the time scale of the hard interaction is very short compared to the time it would take for the quark to readjust itself. As a result, if we could perform some measurement of the quark state using, say, a virtual-photon probe, we could then use this knowledge on the state of the quark to perform predictions for the interaction of the proton

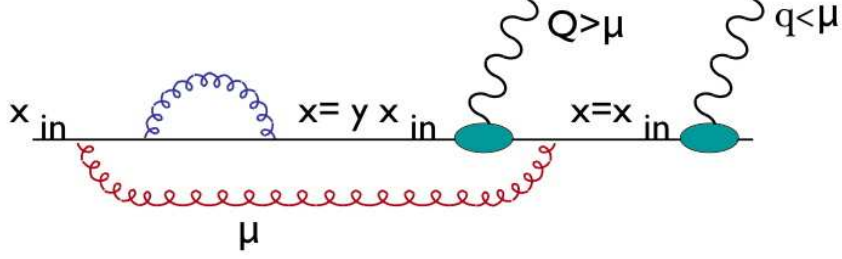


Fig. 5: Scale dependence of the gluon emission during a hard collision

with any other probe (e.g., a virtual W or even a gluon from an opposite beam of hadrons). This is the essence of the universality of the parton distributions.

The above picture leads to an important observation. It appears in fact that which gluons are reabsorbed and which ones are not depends on the scale Q of the hard probe. As a result, the parton density $f(x)$ appears to depend on Q . This is illustrated in Fig. 5. The gluon emitted at a scale μ has a lifetime short enough to be reabsorbed before a collision with a photon of virtuality $Q < \mu$, but too long for a photon of virtuality $Q > \mu$. When going from μ to Q , therefore, the partonic density $f(x)$ changes. We can easily describe this variation as follows:

$$f(x, Q) = f(x, \mu) + \int_x^1 dx_{\text{in}} f(x_{\text{in}}, \mu) \int_{\mu}^Q dq^2 \int_0^1 dy \mathcal{P}(y, q^2) \delta(x - yx_{\text{in}}). \quad (49)$$

Here we obtain the density at the scale Q by adding to $f(x)$ at the scale μ (which we label $f(x, \mu)$) all the quarks with momentum $x_{\text{in}} > x$, which retain a momentum fraction $x = y/x_{\text{in}}$ by emitting a gluon. The function $\mathcal{P}(y, Q^2)$ describes the ‘probability’ that the quark emits a gluon at a scale Q , keeping a fraction y of its momentum. This function does not depend on the details of the hard process, it simply describes the radiation of a quark subject to an interaction with virtuality Q . Since $f(x, Q)$ does not depend upon μ (μ is just used as a reference scale to construct our argument), the total derivative of the right-hand side with respect to μ should vanish, leading to the following equation:

$$\frac{df(x, Q)}{d\mu^2} = 0 \quad \Rightarrow \quad \frac{df(x, \mu)}{d\mu^2} = \int_x^1 \frac{dy}{y} f(y, \mu) \mathcal{P}(x/y, \mu^2). \quad (50)$$

One can prove (see Appendix B) that

$$\mathcal{P}(x, Q^2) = \frac{\alpha_s}{2\pi} \frac{1}{Q^2} P(x), \quad (51)$$

from which the Altarelli–Parisi equation follows:

$$\frac{df(x, \mu)}{d \log \mu^2} = \frac{\alpha_s}{2\pi} \int_x^1 \frac{dy}{y} f(y, \mu) P_{qq}(x/y). \quad (52)$$

The so-called splitting function $P_{qq}(x)$ can be calculated in perturbative QCD, and is given in Appendix B. The subscript qq is a convention indicating that x refers to the momentum fraction retained by a quark after emission of a gluon.

More in general, one should consider additional processes. For example, one should include cases in which the quark interacting with the photon comes from the splitting of a gluon. This is shown in Fig. 6: the left diagram is the one we considered above; the right diagram corresponds to processes where an emitted gluon has the time to split into a $q\bar{q}$ pair, and it is one of these quarks which interacts with the photon. The overall evolution equation, including the effect of gluon splitting, is given by

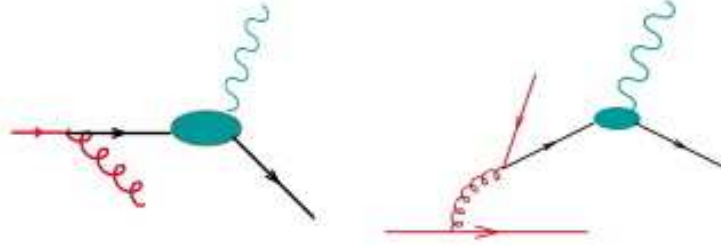


Fig. 6: The processes leading to the evolution of the quark density



Fig. 7: The processes leading to the evolution of the gluon density

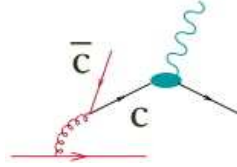


Fig. 8: Gluon evolution leading to a charm-quark content of the proton

$$\frac{dq(x, Q)}{dt} = \frac{\alpha_s}{2\pi} \int_x^1 \frac{dy}{y} \left[q(y, Q) P_{qq}\left(\frac{x}{y}\right) + g(y, Q) P_{qg}\left(\frac{x}{y}\right) \right]. \quad (53)$$

For external probes which couple to gluons (namely an external gluon, coming, for example, from an incoming proton), we have a similar evolution of the gluon density (see Fig. 7):

$$\frac{dg(x, Q)}{dt} = \frac{\alpha_s}{2\pi} \int_x^1 \frac{dy}{y} \left[g(y, Q) P_{gg}\left(\frac{x}{y}\right) + \sum_{q, \bar{q}} q(y, Q) P_{gq}\left(\frac{x}{y}\right) \right]. \quad (54)$$

3.2 Example: the charm content of the proton

If the virtuality of the external probe is large enough, the time scale of the hard interaction is so short that gluon fluctuations into virtual heavy-quark states can be intercepted, and the virtual heavy quarks (charm quarks in our example) can be brought on-shell via the interaction with the photon (see Fig. 8). To the external photon, it will therefore appear as if the proton contained some charm. Its density can be calculated using the Altarelli–Parisi equation, assuming that the heavy-quark density itself is 0 at $Q \sim m_c$, and builds up according to the evolution equation

$$\frac{dc(x, Q)}{dt} = \frac{\alpha_s}{2\pi} \int_x^1 \frac{dy}{y} g(y, Q) P_{qg}\left(\frac{x}{y}\right). \quad (55)$$

Assuming a gluon density behaving like $g(x, Q) \sim A/x$, which is a first approximation to a bremsstrahlung spectrum, we can easily calculate

$$\frac{dc(x, Q)}{dt} = \frac{\alpha_s}{2\pi} \int_x^1 \frac{dy}{y} g(x/y, Q) P_{qg}(y) = \frac{\alpha_s}{2\pi} \int_x^1 dy \frac{A}{x} \frac{1}{2} [y^2 + (1-y)^2]$$

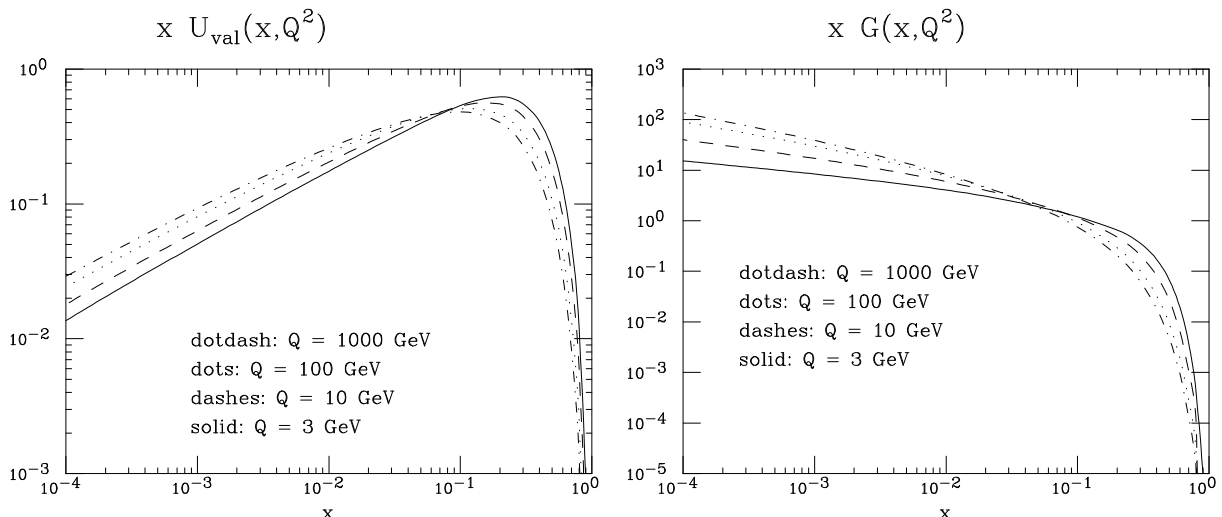


Fig. 9: Left: Valence up-quark momentum-density distribution, for different scales Q . Right: gluon momentum-density distribution.

$$= \frac{\alpha_s}{6\pi} \frac{A}{x} c(x, Q) \sim \frac{\alpha_s}{6\pi} \log\left(\frac{Q^2}{m_c^2}\right) g(x, Q). \quad (56)$$

The charm density is therefore proportional to the gluon density, up to an overall factor proportional to α_s . When Q becomes very large, the effect of the quark mass becomes subleading, and we expect all sea quarks to reach asymptotically the same density!

3.3 Examples of parton density evolution

Figure 9 (left) describes the up-quark valence momentum density at different scales Q . Note the softening at large scales, and the clear $\log Q^2$ evolution. As Q^2 grows, the valence quarks emit more and more radiation, since their deceleration is larger. They therefore lose more momentum to the emitted gluons, and their spectrum becomes softer. The most likely momentum fraction carried by a valence up-quark in the proton goes from $x \sim 20\%$ at $Q = 3$ GeV, to $x \lesssim 10\%$ at $Q = 1000$ GeV. Notice finally that the density vanishes at small x .

Figure 9 (right) shows the gluon momentum density at different scales Q . Their density grows at small x , with an approximate $g(x) \sim 1/x^{1+\delta}$ behaviour, and $\delta > 0$ slowly increasing at large Q^2 . This low- x growth is due to the $1/x$ emission probability for the radiation of gluons, which was discussed in the previous lecture and which is represented by the $1/x$ factors in the $P_{gq}(x)$ and $P_{gg}(x)$ splitting functions. As Q^2 grows we find an increasing number of gluons at small x , as a result of the increased radiation off quarks, as well as off the harder gluons.

Figure 10 (left) shows the evolution of the up-quark *sea* momentum density. Shape and evolution match those of the gluon density, a consequence of the fact that sea quarks come from the splitting of gluons. Since the gluon-splitting probability is proportional to α_s , the approximate ratio *sea*/gluon ~ 0.1 which can be obtained by comparing Figs. 9 (right) and 10 (left) is perfectly justified.

Finally, the momentum densities for gluons, up-sea, charm and up-valence distributions are shown in Fig. 10 (right) for $Q = 1000$ GeV. Note here that u_{sea} and charm are approximately the same at very large Q and small x , as anticipated in the previous subsection. The proton momentum is mostly carried by valence quarks and by gluons. The contribution of sea quarks is negligible.

Parton densities are extracted from experimental data. Their determination is therefore subject to the statistical and systematic uncertainties of the experiments and of the theoretical analysis (e.g., the treatment of non-perturbative effects, the impact of missing higher-order perturbative corrections).

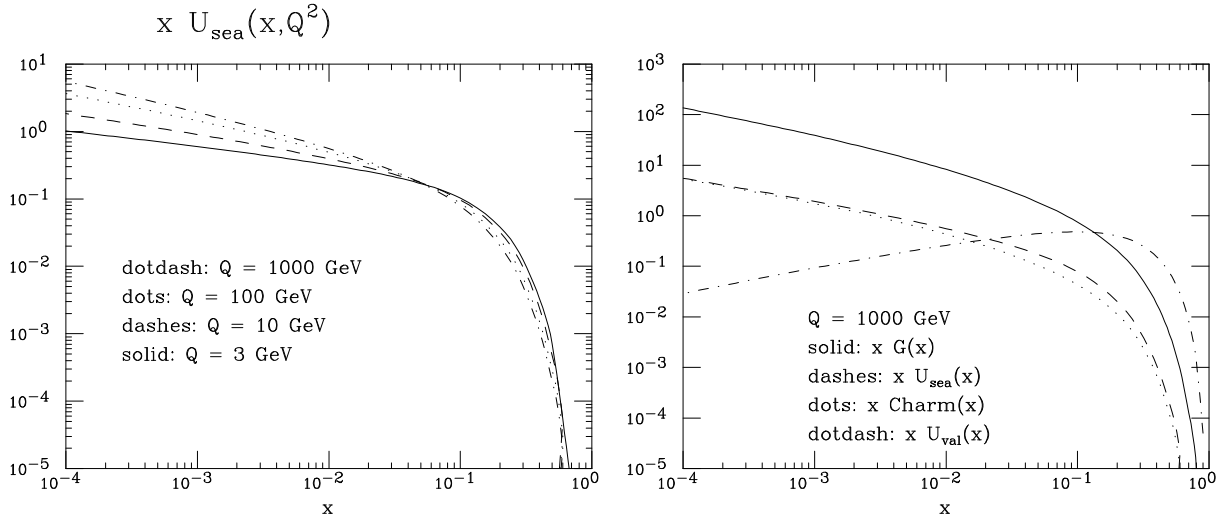


Fig. 10: Left: Sea up-quark momentum-density distribution, for different scales Q . Right: Momentum-density distribution for several parton species, at $Q = 1000$ GeV.

Techniques have been introduced recently to take into account these uncertainties, and to evaluate their impact on concrete observables. A summary of such an analysis is given in Figs. 11 (for the Tevatron) and 12 (for the LHC). What is plotted is the uncertainty bands for partonic luminosities corresponding to various initial-state channels, such as gg , qg or $q\bar{q}$. The partonic flux is given as a function of \hat{s} , the partonic centre-of-mass invariant mass. Obvious features include the growth of uncertainty of the gg density at large mass, corresponding to the lack of data covering the large- x region of the gluon density. As a result of this, notice for example that the uncertainty in the $gg \rightarrow t\bar{t}$ production rate at the LHC is smaller than at the Tevatron, since the relative range of mass (just above $2m_t \sim 350$ GeV) corresponds at the LHC to gluon densities in better explored regions of x .

4 The evolution of quarks and gluons

We discussed in the previous section the initial-state evolution of quarks and gluons as the proton approaches the hard collision. We study here how quarks and gluons evolve, and finally transform into hadrons, neutralizing their colours. We start by considering the simplest case, e^+e^- collisions, which provide the cleanest environment in which to study applications of QCD at high energy. This is the place where theoretical calculations have today reached their best accuracy, and where experimental data are the most precise, especially thanks to the huge statistics accumulated by LEP, LEP2 and SLC. The key process is the annihilation of the e^+e^- pair into a virtual photon or Z^0 boson, which will subsequently decay to a $q\bar{q}$ pair. e^+e^- collisions have therefore the big advantage of providing an almost point-like source of quark pairs, so that, contrary to the case of interactions involving hadrons in the initial state, we at least know very precisely the state of the quarks at the beginning of the interaction process.

Nevertheless, it is by no means obvious that this information is sufficient to predict the properties of the hadronic final state. We know that this final state is clearly not simply a $q\bar{q}$ pair, but some high-multiplicity set of hadrons. For example, the average multiplicity of charged hadrons in the decay of a Z^0 is approximately 20! It is therefore not obvious that a calculation done using the simple picture $e^+e^- \rightarrow q\bar{q}$ will have anything to do with reality. For example, one may wonder why we do not need to calculate $\sigma(e^+e^- \rightarrow q\bar{q}g \dots g \dots)$ for all possible gluon multiplicities to get an accurate estimate of $\sigma(e^+e^- \rightarrow \text{hadrons})$. And since in any case the final state is not made of q 's and g 's, but of π 's, K 's, ρ 's, etc., why would $\sigma(e^+e^- \rightarrow q\bar{q}g \dots g)$ be enough?

The solution to this puzzle lies both in time and energy scales, and in the dynamics of QCD. When

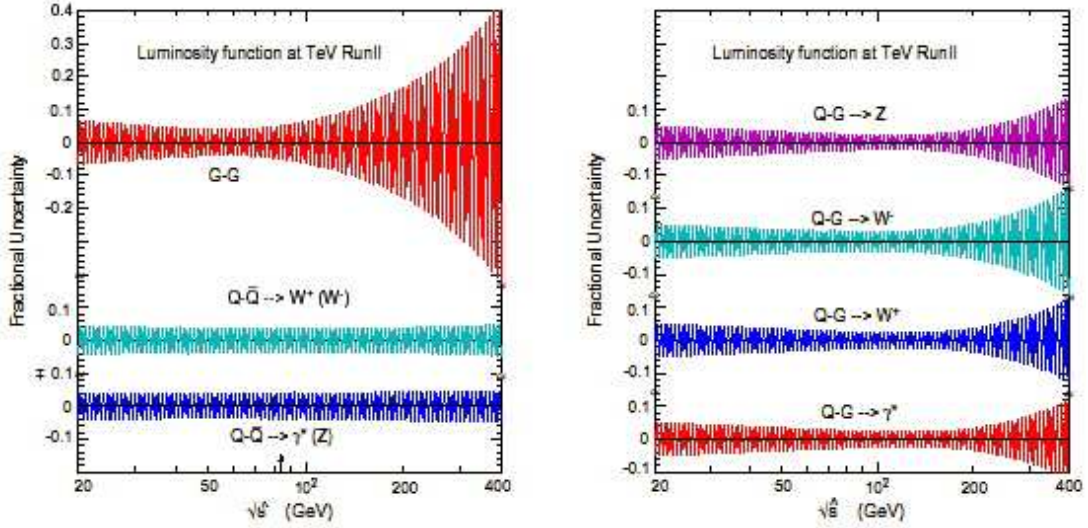


Fig. 11: Uncertainty in the parton luminosity functions at the Tevatron

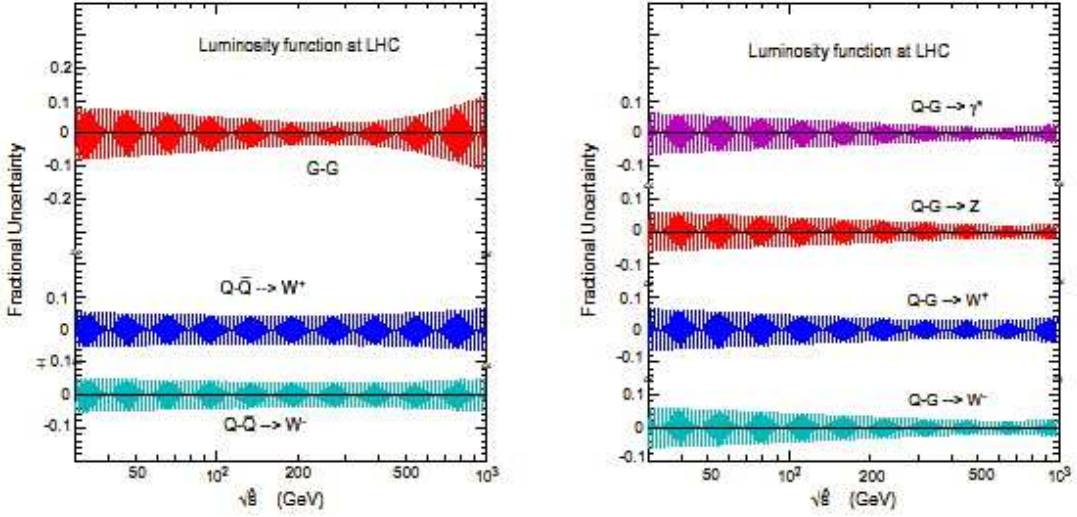


Fig. 12: Uncertainty in the parton luminosity functions at the LHC

the $q\bar{q}$ pair is produced, the force binding q and \bar{q} is proportional to $\alpha_s(s)$ (\sqrt{s} being the e^+e^- centre-of-mass energy). Therefore it is weak, and q and \bar{q} behave to good approximation like free particles. The radiation emitted in the first instants after the pair creation is also perturbative, and it will stay so until a time after creation of the order of $(1 \text{ GeV})^{-1}$, when radiation with wavelengths $\gtrsim (1 \text{ GeV})^{-1}$ starts being emitted. At this scale the coupling constant is large, and non-perturbative phenomena and hadronization start playing a role. However, as we will show, colour emission during the perturbative evolution organizes itself in such a way as to form colour-neutral, low-mass parton clusters highly localized in phase-space. As a result, the complete colour-neutralization (i.e., the hadronization) does not involve long-range interactions between partons far away in phase-space. This is very important, because the forces acting among coloured objects at this time scale would be huge. If the perturbative evolution were to separate far apart colour-singlet $q\bar{q}$ pairs, the final-state interactions taking place during the hadronization phase would totally upset the structure of the final state. As an additional result of this ‘pre-confining’ evolution, memory of where the local colour-neutral clusters came from is totally lost. So we expect the properties of hadronization to be universal: a model that describes hadronization at a given energy will work equally well at some other energy. Furthermore, so much time has passed since

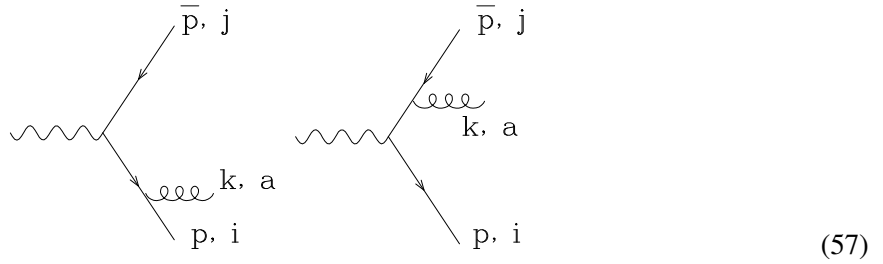
the original $q\bar{q}$ creation, that the hadronization phase cannot significantly affect the total hadron production rate. Perturbative corrections due to the emission of the first hard partons should be calculable in perturbation theory (PT), providing a finite, meaningful cross-section.

The nature of non-perturbative corrections to this picture can be explored. One can prove for example that the leading correction to the total rate $R_{e^+e^-}$ is of order F/s^2 , where $F \propto \langle 0 | \alpha_s F_{\mu\nu}^a F^{\mu\nu a} | 0 \rangle$ is the so-called gluon condensate. Since $F \sim \mathcal{O}(1 \text{ GeV}^4)$, these NP corrections are usually very small. For example, they are of $\mathcal{O}(10^{-8})$ at the Z^0 peak! Corrections scaling like Λ^2/s or Λ/\sqrt{s} can nevertheless appear in other less inclusive quantities, such as event shapes or fragmentation functions.

We now come back to the perturbative evolution, and will devote the first part of this lecture to justifying the picture given above. In Appendix C we shall discuss some applications, including jet cross-sections and shape variables.

4.1 Soft gluon emission

Emission of soft gluons plays a fundamental rôle in the evolution of the final state [6, 15]. Soft gluons are emitted with large probability, since the emission spectrum behaves like dE/E , typical of bremsstrahlung as familiar in QED. They provide the seed for the bulk of the final-state multiplicity of hadrons. The study of soft-gluon emission is simplified by the simplicity of their couplings. Being soft (i.e., long wavelength) they are insensitive to the details of the very-short-distance dynamics: they cannot distinguish features of the interactions which take place on time scales shorter than their wavelength. They are also insensitive to the spin of the partons: the only feature they are sensitive to is the colour charge. To prove this let us consider soft-gluon emission in the $q\bar{q}$ decay of an off-shell photon:

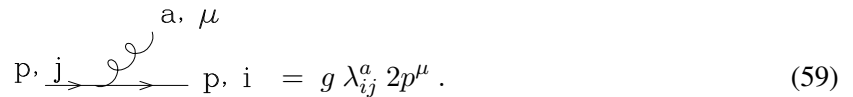


$$\begin{aligned}
 A_{\text{soft}} &= \bar{u}(p)\epsilon(k)(ig) \frac{-i}{\not{p} + \not{k}} \Gamma^\mu v(\bar{p}) \lambda_{ij}^a + \bar{u}(p) \Gamma^\mu \frac{i}{\not{p} + \not{k}} (ig)\epsilon(k) v(\bar{p}) \lambda_{ij}^a \\
 &= \left[\frac{g}{2p \cdot k} \bar{u}(p)\epsilon(k) (\not{p} + \not{k}) \Gamma^\mu v(\bar{p}) - \frac{g}{2\bar{p} \cdot k} \bar{u}(p) \Gamma^\mu (\not{p} + \not{k}) \epsilon(k) v(\bar{p}) \right] \lambda_{ij}^a .
 \end{aligned}$$

I used the generic symbol Γ_μ to describe the interaction vertex with the photon to stress the fact that the following manipulations are independent of the specific form of Γ_μ . In particular, Γ_μ can represent an arbitrarily complicated vertex form factor. Neglecting the factors of \not{k} in the numerators (since $k \ll p, \bar{p}$, by definition of soft) and using the Dirac equations, we get

$$A_{\text{soft}} = g \lambda_{ij}^a \left(\frac{p \cdot \epsilon}{p \cdot k} - \frac{\bar{p} \cdot \epsilon}{\bar{p} \cdot k} \right) A_{\text{Born}} . \quad (58)$$

We then conclude that soft-gluon emission factorizes into the product of an emission factor, times the Born-level amplitude. From this exercise, one can extract general Feynman rules for soft-gluon emission:



4.2 Angular ordering for soft-gluon emission

The results presented above have important consequences for the perturbative evolution of the quarks. A key property of the soft-gluon emission is the so-called *angular ordering*. This phenomenon consists in the continuous reduction of the opening angle at which successive soft gluons are emitted by the evolving quark. As a result, this radiation is confined within smaller and smaller cones around the quark direction, and the final state will look like a collimated jet of partons. In addition, the structure of the colour flow during the jet evolution forces the $q\bar{q}$ pairs which are in a colour-singlet state to be close in phase-space, thereby achieving the pre-confinement of colour-singlet clusters alluded to at the beginning of this section.

Let us start by proving the property of colour ordering. Consider the $q\bar{q}$ pair produced by the decay of a rapidly moving virtual photon. The amplitude for the emission of a soft gluon was given in Eq. (58). Squaring, summing over colours and including the gluon phase-space we get the following result:

$$\begin{aligned}
 d\sigma_g &= \sum |A_{\text{soft}}|^2 \frac{d^3k}{(2\pi)^3 2k^0} \sum |A_0|^2 \frac{-2p^\mu \bar{p}^\nu}{(pk)(\bar{p}k)} g^2 \sum \epsilon_\mu \epsilon_\nu^* \frac{d^3k}{(2\pi)^3 2k^0} \\
 &= d\sigma_0 \frac{2(p\bar{p})}{(pk)(\bar{p}k)} g^2 C_F \left(\frac{d\phi}{2\pi} \right) \frac{k^0 dk^0}{8\pi^2} d \cos \theta \\
 &= d\sigma_0 \frac{\alpha_s C_F}{\pi} \frac{dk^0}{k^0} \frac{d\phi}{2\pi} \frac{1 - \cos \theta_{ij}}{(1 - \cos \theta_{ik})(1 - \cos \theta_{jk})} d \cos \theta
 \end{aligned} \tag{66}$$

where $\theta_{\alpha\beta} = \theta_\alpha - \theta_\beta$, and i, j, k refer to the q, \bar{q} and gluon directions, respectively. We can write the following identity:

$$\frac{1 - \cos \theta_{ij}}{(1 - \cos \theta_{ik})(1 - \cos \theta_{jk})} = \frac{1}{2} \left[\frac{\cos \theta_{jk} - \cos \theta_{ij}}{(1 - \cos \theta_{ik})(1 - \cos \theta_{jk})} + \frac{1}{1 - \cos \theta_{ik}} \right] + \frac{1}{2} [i \leftrightarrow j] \equiv W_{(i)} + W_{(j)}. \tag{67}$$

We would like to interpret the two functions $W_{(i)}$ and $W_{(j)}$ as radiation probabilities from the quark and antiquark lines. Each of them is in fact only singular in the limit of gluon emission parallel to the respective quark:

$$W_{(i)} \rightarrow \text{finite if } k \parallel j \text{ (} \cos \theta_{jk} \rightarrow 1 \text{)} \tag{68}$$

$$W_{(j)} \rightarrow \text{finite if } k \parallel i \text{ (} \cos \theta_{ik} \rightarrow 1 \text{)}. \tag{69}$$

The interpretation as probabilities is however limited by the fact that neither $W_{(i)}$ nor $W_{(j)}$ are positive definite. However, you can easily prove that

$$\int \frac{d\phi}{2\pi} W_{(i)} = \begin{cases} \frac{1}{1 - \cos \theta_{ik}} & \text{if } \theta_{ik} < \theta_{ij} \\ 0 & \text{otherwise} \end{cases} \tag{70}$$

where the integral is the azimuthal average around the q direction. A similar result holds for $W_{(j)}$:

$$\int \frac{d\phi}{2\pi} W_{(j)} = \begin{cases} \frac{1}{1 - \cos \theta_{jk}} & \text{if } \theta_{jk} < \theta_{ij} \\ 0 & \text{otherwise} \end{cases}. \tag{71}$$

As a result, the emission of soft gluons outside the two cones obtained by rotating the antiquark direction around the quark's, and vice-versa, averages to 0. Inside the two cones, one can consider the radiation from the emitters as being uncorrelated. In other words, the two colour lines defined by the quark and antiquark currents act as independent emitters, and the quantum coherence (i.e., the effects of interference between the two graphs contributing to the gluon-emission amplitude) is accounted for by constraining the emission to take place within those fixed cones.

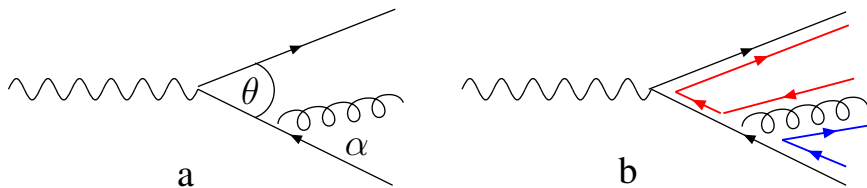


Fig. 13: Radiation off $q\bar{q}$ pair produced by an off-shell photon

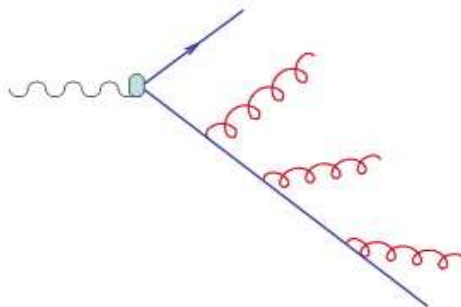


Fig. 14: Collimation of soft gluon emission during the jet evolution

A simple derivation of angular ordering, which more directly exhibits its physical origin, can be obtained as follows. Consider Fig. 13a, which shows a Feynman diagram for the emission of a gluon from a quark line. The quark momentum is denoted by l and the gluon momentum by k ; θ is the opening angle between the quark and antiquark, and α is the angle between the nearest quark and the emitted gluon. We will work in the double-log enhanced soft $k^0 \ll l^0$ and collinear $\alpha \ll 1$ region. The internal quark propagator $p = (l + k)$ is off-shell, setting the time scale for the gluon emission:

$$\Delta t \simeq \frac{1}{\Delta E} = \frac{l^0}{(k+l)^2} \quad \rightarrow \quad \Delta t \simeq \frac{1}{k^0 \alpha^2}. \quad (72)$$

In order to resolve the quarks, the transverse wavelength of the gluon $\lambda_{\perp} = 1/E_{\perp}$ must be smaller than the separation between the quarks $b(t) \simeq \theta \Delta t$, giving the constraint $1/(\alpha k^0) < \theta \Delta t$. Using the results of Eq. (72) for Δt , we arrive at the angular ordering constraint $\alpha < \theta$. Gluon emissions at an angle smaller than θ can resolve the two individual colour quarks and are allowed; emissions at greater angles do not see the colour charge and are therefore suppressed. In processes involving more partons, the angle θ is defined not by the nearest parton, but by the colour connected parton (e.g., the parton that forms a colour singlet with the emitting parton). Figure 13b shows the colour connections for the $q\bar{q}$ event after the gluon is emitted. Colour lines begin on quarks and end on antiquarks. Because gluons are colour octets, they contain the beginning of one line and the end of another.

If one now repeats the exercise for emission of one additional gluon, one will find the same angular constraint, but this time applied to the colour lines defined by the previously established *antenna*. As shown in the previous subsection, the $q\bar{q}g$ state can be decomposed at the leading order in $1/N$ into two independent emitters: one given by the colour line flowing from the gluon to the quark, the other given by the colour line flowing from the antiquark to the gluon. So the emission of the additional gluon will be constrained to take place either within the cone formed by the quark and the gluon, or within the cone formed by the gluon and the antiquark. Either way, the emission angle will be smaller than the angle of the first gluon emission. This leads to the concept of angular ordering, with successive emission of soft gluons taking place within cones which get smaller and smaller, as in Fig. 14.

The fact that colour always flows directly from the emitting parton to the emitted one, the colli-

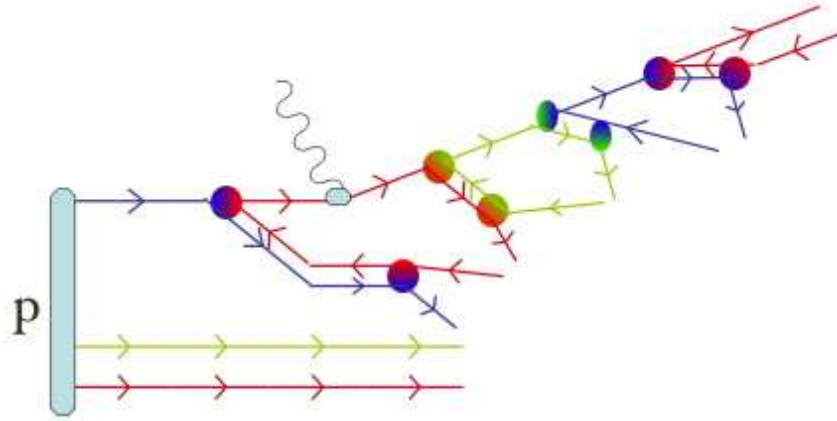


Fig. 15: The colour flow diagram for a deep-inelastic scattering event



Fig. 16: Charge transfer in a dielectric medium, via a sequence of local polarizations

mation of the jet, and the softening of the radiation emitted at later stages ensure that partons forming a colour-singlet cluster are close in phase-space. As a result, hadronization (the non-perturbative process that will bind together colour-singlet parton pairs) takes place locally inside the jet and is not a long-distance phenomenon connecting partons far away in the evolution tree: only pairs of nearby partons are involved. In particular, there is no direct link between the precise nature of the hard process and the hadronization. These two phases are totally decoupled and, as in the case of the partonic densities, one can infer that hadronization factorizes from the hard process and can be described in a universal (i.e., hard-process independent) fashion. The inclusive properties of jets (particle multiplicity, jet mass, jet broadening, etc.) are independent of the hadronization model, up to corrections of order $(\Lambda/\sqrt{s})^n$ (for some integer power n , which depends on the observable), with $\Lambda \lesssim 1$ GeV.

The final picture, in the case of a DIS event, appears therefore as in Fig. 15. After being deflected by the photon, the struck quark emits the first gluon, which takes away the quark colour and passes on its own anticolour to the escaping quark. This gluon is therefore colour-connected with the last gluon emitted before the hard interaction. As the final-state quark continues its evolution, more and more gluons are emitted, each time leaving their colour behind and transmitting their anticolour to the emerging quark. Angular ordering forces all these gluons to be close in phase-space, until the evolution is stopped once the virtuality of the quark becomes of the order of the strong-interaction scale. The colour of the quark is left behind, and when hadronization takes over it is only the nearby colour-connected gluons which are transformed, with a phenomenological model, in hadrons. This mechanism for the transfer of colour across subsequent gluon emissions is similar to what happens when we place a charge near the surface of a dielectric medium. This will become polarized, and a charge will appear on the opposite end of the medium. The appearance of the charge is the result of a sequence of local charge shifts, whereby neighbouring atoms get polarized, as in Fig. 16.

5 Applications to hadronic collisions

In hadronic collisions, all phenomena are QCD-related. The dynamics is more complex than in e^+e^- or DIS, since both beam and target have a non-trivial partonic structure. As a result, calculations (and experimental analyses) are more complicated. QCD phenomenology is however much richer, and the higher energies available in hadronic collisions allow us to probe the structure of the proton and of its constituents at the smallest scales attainable in a laboratory.

Contrary to the case of e^+e^- and lepton–hadron collisions, where calculations are routinely available up to next-to-next-to-leading order (NNLO) accuracy, theoretical calculations for hadronic collisions are available at best with next-to-leading-order (NLO) accuracy. The only exception is the case of Drell–Yan production, where NNLO results are known for the total cross-sections. So we generally have relatively small precision in the theoretical predictions, and theoretical uncertainties which are large when compared to LEP or HERA.

However, $p\bar{p}$ collider physics is primarily *discovery* physics, rather than precision physics. (There are exceptions, such as the measurements of the W mass and of the properties of b -hadrons; but these are not QCD-related measurements.) As such, knowledge of QCD is essential both for the estimate of the expected signals, and for the evaluation of the backgrounds. Tests of QCD in $p\bar{p}$ collisions confirm our understanding of perturbation theory, or, when they fail, point to areas where our approximations need to be improved. (see, e.g., the theory advances prompted by the measurements of ψ production by CDF at the Tevatron!).

Finally, a reliable theoretical control over the details of production dynamics allows one to extract important information on the structure of the proton (parton densities) in regions of Q^2 and x otherwise inaccessible. Control of QCD at the current machines (the Tevatron at Fermilab) is therefore essential for the extrapolation of predictions to higher energies (say for applications at the future LHC, at CERN).

The key ingredients for the calculation of production rates and distributions in hadronic collisions are

- the matrix elements for the hard, partonic process (e.g., $gg \rightarrow gg, gg \rightarrow b\bar{b}, q\bar{q}' \rightarrow W, \dots$);
- the hadronic parton densities, discussed in the previous lecture.

Then the production rate for a given final state H is given by a factorization formula similar to the one used to describe DIS:

$$d\sigma(p\bar{p} \rightarrow H + X) = \int dx_1 dx_2 \sum_{i,j} f_i(x_1, Q) f_j(x_2, Q) d\hat{\sigma}(ij \rightarrow H) \quad (73)$$

where the parton densities f_i are evaluated at a scale Q typical of the hard process under consideration. For example $Q \simeq M_{\text{DY}}$ for production of a Drell–Yan pair, $Q \simeq E_{\text{T}}$ for high transverse-energy (E_{T}) jets, $Q^2 \simeq p_{\text{T}}^2 + m_Q^2$ for high- p_{T} heavy quarks, etc.

In this lecture we will briefly explore two of the QCD phenomena currently studied in hadronic collisions: Drell–Yan, and inclusive jet production. More details can be found in Refs. [4, 8].

5.1 Drell–Yan processes

While the Z boson has been recently studied with great precision by the LEP experiments, it was actually discovered, together with the W boson, by the CERN experiments UA1 and UA2 in $p\bar{p}$ collisions. W physics is now being studied in great detail at LEP2, but the best direct measurements of its mass by a single group still belong to $p\bar{p}$ experiments (CDF and D0 at the Tevatron). Even after the ultimate luminosity will have been accumulated at LEP2, with a great improvement in the determination of the parameters of the W boson, the monopoly of W studies will immediately return to hadron colliders, with the Tevatron data-taking resuming in the year 2000, and later on with the start of the LHC experiments.

Precision measurements of W production in hadronic collisions are important for several reasons:

- this is the only process in hadronic collisions which is known to NNLO accuracy;
- the rapidity distribution of the charged leptons from W decays is sensitive to the ratio of the up- and down-quark densities, and can contribute to our understanding of the proton structure;
- deviations from the expected production rates of highly virtual W 's ($p\bar{p} \rightarrow W^* \rightarrow e\nu$) are a possible signal of the existence of new W bosons, and therefore of new gauge interactions.

The partonic cross-section for the production of a W boson from the annihilation of a $q\bar{q}$ pair can be easily calculated, giving the following result [4, 8]:

$$\hat{\sigma}(q_i\bar{q}_j \rightarrow W) = \pi \frac{\sqrt{2}}{3} |V_{ij}|^2 G_F M_W^2 \delta(\hat{s} - M_W^2) = A_{ij} M_W^2 \delta(\hat{s} - M_W^2) \quad (74)$$

where \hat{s} is partonic centre-of-mass (c.m.) energy squared, and V_{ij} is the element of the Cabibbo–Kobayashi–Maskawa matrix. The delta function comes from the $2 \rightarrow 1$ phase-space, which forces the c.m. energy of the initial state to coincide with the W mass. It is useful to introduce the two variables

$$\tau = \frac{\hat{s}}{S_{\text{had}}} \equiv x_1 x_2 \quad (75)$$

$$y = \frac{1}{2} \log \left(\frac{E_W + p_W^z}{E_W - p_W^z} \right) \equiv \frac{1}{2} \log \left(\frac{x_1}{x_2} \right), \quad (76)$$

where S_{had} is the hadronic c.m. energy squared. The variable y is called *rapidity*. For slowly moving objects it reduces to the standard velocity, but, unlike the velocity, it transforms additively even at high energies under Lorentz boosts along the direction of motion. Written in terms of τ and y , the integration measure over the initial-state parton momenta becomes $dx_1 dx_2 = d\tau dy$. Using this expression and Eq. (74) in Eq. (73), we obtain the following result for the leading-order total W production cross-section:

$$\sigma_{\text{DY}} = \sum_{i,j} \frac{\pi A_{ij}}{M_W^2} \tau \int_{\tau}^1 \frac{dx}{x} f_i(x) f_j \left(\frac{\tau}{x} \right) \equiv \sum_{i,j} \frac{\pi A_{ij}}{M_W^2} \tau \mathcal{L}_{ij}(\tau) \quad (77)$$

where the function $\mathcal{L}_{ij}(\tau)$ is usually called *partonic luminosity*. In the case of $u\bar{d}$ collisions, the overall factor in front of this expression has a value of approximately 6.5 nb. It is interesting to study the partonic luminosity as a function of the hadronic c.m. energy. This can be done by taking a simple approximation for the parton densities. Following the indications of the figures presented in the previous lecture, we shall assume that $f_i(x) \sim 1/x^{1+\delta}$, with $\delta < 1$. Then

$$\mathcal{L}(\tau) = \int_{\tau}^1 \frac{dx}{x} \frac{1}{x^{1+\delta}} \left(\frac{x}{\tau} \right)^{1+\delta} = \frac{1}{\tau^{1+\delta}} \int_{\tau}^1 \frac{dx}{x} = \frac{1}{\tau^{1+\delta}} \log \left(\frac{1}{\tau} \right) \quad (78)$$

and

$$\sigma_W \sim \tau^{-\delta} \log \left(\frac{1}{\tau} \right) = \left(\frac{S_{\text{had}}}{M_W^2} \right)^{\delta} \log \left(\frac{S_{\text{had}}}{M_W^2} \right). \quad (79)$$

The Drell-Yan cross-section grows therefore at least logarithmically with the hadronic c.m. energy. This is to be compared with the behaviour of the Z production cross-section in e^+e^- collisions, which is steeply diminishing for values of s well above the production threshold. The reason for the different behaviour in hadronic collisions is that while the energy of the hadronic initial state grows, it will always be possible to find partons inside the hadrons with the appropriate energy to produce the W directly on-shell. The number of partons available for the production of a W is furthermore increasing with the increase in hadronic energy, since the larger the hadron energy, the smaller will be the value of hadron

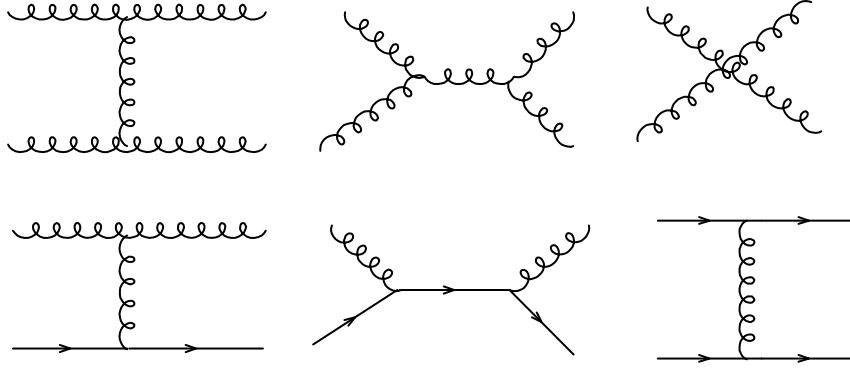


Fig. 18: Representative diagrams for the production of jet pairs in hadronic collisions

5.2 W rapidity asymmetry

The measurement of the charge asymmetry in the rapidity distribution of W bosons produced in $p\bar{p}$ collisions can provide an important measurement of the ratio of the u -quark and d -quark momentum distributions. Using the formulas provided above, you can in fact easily check as an exercise that

$$\frac{d\sigma_{W^+}}{dy} \propto f_u^p(x_1) f_{\bar{d}}^{\bar{p}}(x_2) + f_{\bar{d}}^p(x_1) f_u^{\bar{p}}(x_2) \quad (80)$$

$$\frac{d\sigma_{W^-}}{dy} \propto f_u^p(x_1) f_{\bar{d}}^{\bar{p}}(x_2) + f_d^p(x_1) f_u^{\bar{p}}(x_2). \quad (81)$$

We can then construct the following charge asymmetry (assuming the dominance of the quark densities over the antiquark ones, which is valid in the kinematical region of interest for W production at the Tevatron):

$$A(y) = \frac{\frac{d\sigma_{W^+}}{dy} - \frac{d\sigma_{W^-}}{dy}}{\frac{d\sigma_{W^+}}{dy} + \frac{d\sigma_{W^-}}{dy}} = \frac{f_u^p(x_1) f_d^{\bar{p}}(x_2) - f_d^p(x_1) f_u^{\bar{p}}(x_2)}{f_u^p(x_1) f_d^{\bar{p}}(x_2) + f_d^p(x_1) f_u^{\bar{p}}(x_2)}. \quad (82)$$

Setting $f_d(x) = f_u(x) R(x)$, we then get

$$A(y) = \frac{R(x_2) - R(x_1)}{R(x_2) + R(x_1)}, \quad (83)$$

which measures the $R(x)$ ratio since $x_{1,2}$ are known in principle from the kinematics: $x_{1,2} = \sqrt{\tau} \exp(\pm y)$.² The current CDF data provide the most accurate measurement to date of this quantity (see Ref. [8]).

5.3 Jet production

Jet production is the hard process with the largest rate in hadronic collisions. For example, the cross-section for producing at the Tevatron ($\sqrt{S_{\text{had}}} = 1.8$ TeV) jets of transverse energy $E_T^{\text{jet}} \lesssim 50$ GeV is of the order of a μb . This means 50 events per second at the luminosities available at the Tevatron. The data collected at the Tevatron so far extend all the way up to the E_T values of the order of 450 GeV. These events are generated by collisions among partons which carry over 50% of the available $p\bar{p}$ energy, and allow us to probe the shortest distances ever reached. The leading mechanisms for jet production are shown in Fig. 18.

The two-jet inclusive cross-section can be obtained from the formula

$$d\sigma = \sum_{ijkl} dx_1 dx_2 f_i^{(H_1)}(x_1, \mu) f_j^{(H_2)}(x_2, \mu) \frac{d\hat{\sigma}_{ij \rightarrow k+l}}{d\Phi_2} d\Phi_2, \quad (84)$$

²In practice one cannot determine $x_{1,2}$ with arbitrary precision on an event-by-event basis, since the longitudinal momentum of the neutrino cannot be easily measured. The actual measurement is therefore done by studying the charge asymmetry in the rapidity distribution of the charged lepton.

which has to be expressed in terms of the rapidity and transverse momentum of the quarks (or jets) in order to make contact with physical reality. The two-particle phase-space is given by

$$d\Phi_2 = \frac{d^3k}{2k^0(2\pi)^3} 2\pi \delta [(p_1 + p_2 - k)^2] , \quad (85)$$

and, in the c.m. of the colliding partons, we get

$$d\Phi_2 = \frac{1}{2(2\pi)^2} d^2k_T dy 2\delta [\hat{s} - 4(k^0)^2] , \quad (86)$$

where k_T is the transverse momentum of the final-state partons. Here y is the rapidity of the produced parton in the parton c.m. frame. It is given by

$$y = \frac{y_1 - y_2}{2} \quad (87)$$

where y_1 and y_2 are the rapidities of the produced partons in the laboratory frame (in fact, in any frame). One also introduces

$$y_0 = \frac{y_1 + y_2}{2} = \frac{1}{2} \log \frac{x_1}{x_2} , \quad \tau = \frac{\hat{s}}{S_{\text{had}}} = x_1 x_2 . \quad (88)$$

We have

$$dx_1 dx_2 = dy_0 d\tau . \quad (89)$$

We obtain

$$d\sigma = \sum_{ijkl} dy_0 \frac{1}{S_{\text{had}}} f_i^{(H_1)}(x_1, \mu) f_j^{(H_2)}(x_2, \mu) \frac{d\hat{\sigma}_{ij \rightarrow k+l}}{d\Phi_2} \frac{1}{2(2\pi)^2} 2 dy d^2k_T \quad (90)$$

which can also be written as

$$\frac{d\sigma}{dy_1 dy_2 d^2k_T} = \frac{1}{S_{\text{had}} 2(2\pi)^2} \sum_{ijkl} f_i^{(H_1)}(x_1, \mu) f_j^{(H_2)}(x_2, \mu) \frac{d\hat{\sigma}_{ij \rightarrow k+l}}{d\Phi_2} . \quad (91)$$

The variables x_1, x_2 can be obtained from y_1, y_2 and k_T from the equations

$$y_0 = \frac{y_1 + y_2}{2} \quad (92)$$

$$y = \frac{y_1 - y_2}{2} \quad (93)$$

$$x_T = \frac{2k_T}{\sqrt{S_{\text{had}}}} \quad (94)$$

$$x_1 = x_T e^{y_0} \cosh y \quad (95)$$

$$x_2 = x_T e^{-y_0} \cosh y . \quad (96)$$

For the partonic variables, we need \hat{s} and the scattering angle in the parton c.m. frame θ , since

$$t = -\frac{\hat{s}}{2} (1 - \cos \theta) , \quad u = -\frac{\hat{s}}{2} (1 + \cos \theta) . \quad (97)$$

Neglecting the parton masses, you can show that the rapidity can also be written as

$$y = -\log \tan \frac{\theta}{2} \equiv \eta , \quad (98)$$

with η usually being referred to as pseudorapidity.

The leading-order Born cross-sections for parton-parton scattering are reported in Table 1.

Table 1: Cross-sections for light parton scattering. The notation is $p_1 p_2 \rightarrow kl$, $\hat{s} = (p_1 + p_2)^2$, $\hat{t} = (p_1 - k)^2$, $\hat{u} = (p_1 - l)^2$.

Process	$\frac{d\hat{\sigma}}{d\Phi_2}$
$qq' \rightarrow qq'$	$\frac{1}{2} \frac{4}{2\hat{s}} \frac{\hat{s}^2 + \hat{u}^2}{\hat{t}^2}$
$qq \rightarrow qq$	$\frac{1}{2} \frac{1}{2\hat{s}} \left[\frac{4}{9} \left(\frac{\hat{s}^2 + \hat{u}^2}{\hat{t}^2} + \frac{\hat{s}^2 + \hat{t}^2}{\hat{u}^2} \right) - \frac{8}{27} \frac{\hat{s}^2}{\hat{u}\hat{t}} \right]$
$q\bar{q} \rightarrow q'\bar{q}'$	$\frac{1}{2} \frac{4}{2\hat{s}} \frac{\hat{t}^2 + \hat{u}^2}{\hat{s}^2}$
$q\bar{q} \rightarrow q\bar{q}$	$\frac{1}{2\hat{s}} \left[\frac{4}{9} \left(\frac{\hat{s}^2 + \hat{u}^2}{\hat{t}^2} + \frac{\hat{t}^2 + \hat{u}^2}{\hat{s}^2} \right) - \frac{8}{27} \frac{\hat{u}^2}{\hat{s}\hat{t}} \right]$
$q\bar{q} \rightarrow gg$	$\frac{1}{2} \frac{1}{2\hat{s}} \left[\frac{32}{27} \frac{\hat{t}^2 + \hat{u}^2}{\hat{t}\hat{u}} - \frac{8}{3} \frac{\hat{t}^2 + \hat{u}^2}{\hat{s}^2} \right]$
$gg \rightarrow q\bar{q}$	$\frac{1}{2\hat{s}} \left[\frac{1}{6} \frac{\hat{t}^2 + \hat{u}^2}{\hat{t}\hat{u}} - \frac{3}{8} \frac{\hat{t}^2 + \hat{u}^2}{\hat{s}^2} \right]$
$gg \rightarrow gg$	$\frac{1}{2\hat{s}} \left[-\frac{4}{9} \frac{\hat{s}^2 + \hat{u}^2}{\hat{s}\hat{u}} + \frac{\hat{u}^2 + \hat{s}^2}{\hat{t}^2} \right]$
$gg \rightarrow gg$	$\frac{1}{2} \frac{1}{2\hat{s}} \frac{9}{2} \left(3 - \frac{\hat{t}\hat{u}}{\hat{s}^2} - \frac{\hat{s}\hat{u}}{\hat{t}^2} - \frac{\hat{s}\hat{t}}{\hat{u}^2} \right)$

It is interesting to note that a good approximation to the exact results can be easily obtained by using the soft-gluon techniques introduced in the third lecture. Based on the fact that even at 90° $\min(|t|, |u|)$ does not exceed $s/2$, and that therefore everything else being equal a propagator in the t or u channel contributes to the square of an amplitude four times more than a propagator in the s channel, it is reasonable to assume that the amplitudes are dominated by the diagrams with a gluon exchanged in the t (or u) channel. It is easy to calculate the amplitudes in this limit using the soft-gluon approximation. For example, the amplitude for the exchange of a soft gluon among a qq' pair is given by

$$(\lambda_{ij}^a) (\lambda_{kl}^a) 2p_\mu \frac{1}{t} 2p'_\mu = \lambda_{ij}^a \lambda_{kl}^a \frac{4p \cdot p'}{t} = \frac{2s}{t} \lambda_{ij}^a \lambda_{kl}^a. \quad (99)$$

The p_μ and p'_μ factors represent the coupling of the exchanged gluon to the q and q' quark lines, respectively [see Eq. (59)]. Squaring, and summing and averaging over spins and colours, gives

$$\overline{\sum_{\text{colours, spin}} |M_{qq'}|^2} = \frac{1}{N^2} \left(\frac{N^2 - 1}{4} \right) \frac{4s^2}{t^2} = \frac{8}{9} \frac{s^2}{t^2}. \quad (100)$$

Since for this process the diagram with a t -channel gluon exchange is symmetric for $s \leftrightarrow u$ exchange, and since $u \rightarrow -s$ in the $t \rightarrow 0$ limit, the above result can be rewritten in an explicitly (s, u) symmetric way as

$$\frac{4}{9} \frac{s^2 + u^2}{t^2} \quad (101)$$

which indeed exactly agrees with the result of the exact calculation, as given in Table 1. The corrections which appear from s or u gluon exchange when the quark flavours are the same or when we study a $q\bar{q}$ process are small, as can be seen by comparing the above result with the expressions in the table.

As another example we consider the case of $gg \rightarrow gg$ scattering. The amplitude will be exactly the same as in the $qq' \rightarrow qq'$ case, up to the different colour factors. A simple calculation then gives

$$\overline{\sum_{\text{colours, spin}} |M_{gg}|^2} = \frac{9}{4} \overline{\sum_{\text{colours, spin}} |M_{qq'}|^2} = \frac{s^2 + u^2}{t^2}. \quad (102)$$

The exact result is

$$\frac{u^2 + s^2}{t^2} - \frac{4}{9} \frac{u^2 + s^2}{us} \quad (103)$$

which even at 90° , the point where the t -channel exchange approximation is worst, only differs from this latter by no more than 25%.

As a final example we consider the case of $gg \rightarrow gg$ scattering, which in our approximation gives

$$\overline{\sum} |M_{gg}|^2 = \frac{9}{2} \frac{s^2}{t^2}. \quad (104)$$

By $u \leftrightarrow t$ symmetry, we should expect the simple improvement

$$\overline{\sum} |M_{gg}|^2 \sim \frac{9}{2} \left(\frac{s^2}{t^2} + \frac{s^2}{u^2} \right). \quad (105)$$

This only differs by 20% from the exact result at 90° .

Note that at small t the following relation holds:

$$\hat{\sigma}_{gg} : \hat{\sigma}_{qg} : \hat{\sigma}_{q\bar{q}} = \left(\frac{9}{4} \right) : 1 : \left(\frac{4}{9} \right). \quad (106)$$

The 9/4 factors are simply the ratios of the colour factors for the coupling to gluons of a gluon (C_A) and of a quark (T_F), after including the respective colour-average factors: $(1/(N^2 - 1))$ for the gluon, and $1/N$ for the quark). Using Eq. (106), we can then write

$$d\sigma_{\text{hadr}} = \int dx_1 dx_2 \sum_{i,j} f_i(x_1) f_j(x_2) d\hat{\sigma}_{ij} = \int dx_1 dx_2 F(x_1) F(x_2) d\hat{\sigma}_{gg}(gg \rightarrow \text{jets}) \quad (107)$$

where the object

$$F(x) = f_g(x) + \frac{4}{9} \sum_f [q_f(x) + \bar{q}_f(x)] \quad (108)$$

is usually called the *effective structure function*. This result indicates that the measurement of the inclusive jet cross-section does not allow us in principle to disentangle the independent contribution of the various partonic components of the proton, unless of course one is considering a kinematical region where the production is dominated by a single process. The relative contributions of the different channels, as predicted using the global fits of parton densities available in the literature, are shown in Fig. 19.

Predictions for jet production at colliders are available today at next-to-leading order in QCD. A comparison between these calculations and the available data is given in Figs. 20 and 21. At the Tevatron, jets up to 600 GeV transverse momentum have been observed. That is $x \gtrsim 0.6$ and $Q^2 \simeq 400\,000 \text{ GeV}^2$. This is a domain of x and Q^2 not accessible to HERA. The current agreement between theory and data is excellent over eight orders of magnitude of cross-section, from $E_T \sim 50$ to $E_T \sim 600 \text{ GeV}$. The experimental and theoretical systematic uncertainties, however, become larger than 30% when $E_T \gtrsim 400 \text{ GeV}$, preventing a very accurate test of the smallest scales. More data on jet production at large rapidity will allow us to reduce the PDF uncertainties at large x . The uncertainty in the absolute energy scale remains however a critical and difficult to overcome experimental limitation at the highest energies.

Appendices

A Renormalization, or “Theorists are not afraid of infinities!”

QCD calculations are extremely demanding. Although perturbative, the size of the coupling constant even at rather large values of the exchanged momentum, Q^2 , is such that the convergence of the perturbative expansion is slow. Several orders of perturbation theory are required in order to obtain a good accuracy. The complexity of the calculations grows dramatically with the order of the approximation. As

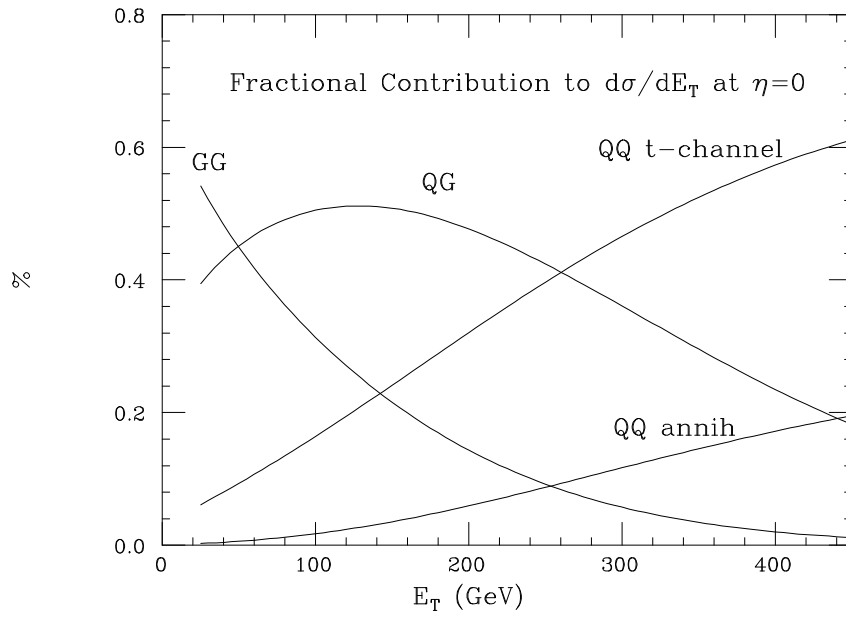


Fig. 19: Relative contribution to the inclusive jet- E_T rates from the different production channels

CDF Run II Preliminary

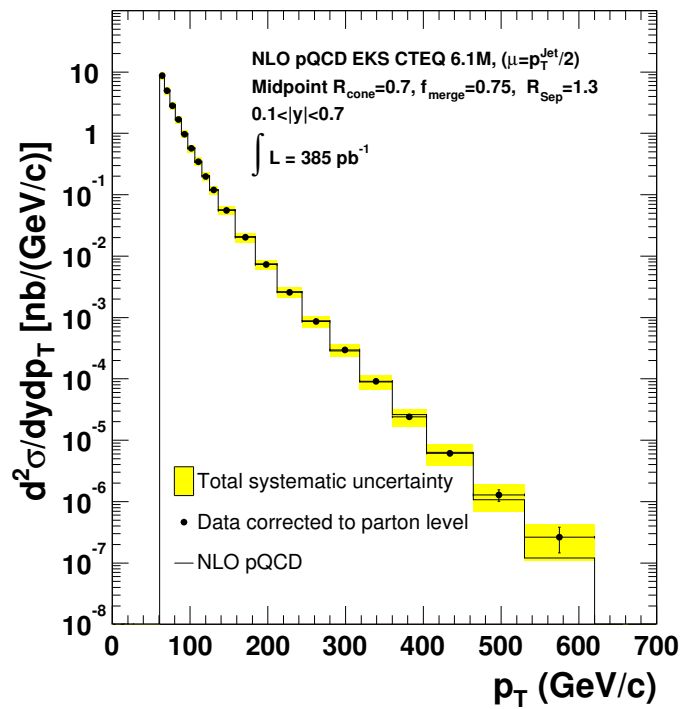


Fig. 20: Inclusive E_T spectra for central jets at the Tevatron

formulas:

$$V(R) = \int \frac{\lambda(r)}{r} dx = \lambda \int_{-\infty}^{+\infty} \frac{dx}{\sqrt{R^2 + x^2}} \quad (\text{A.3})$$

where the integral runs over the position x on the wire. This integral is logarithmically divergent, and the potential is ill-defined. We know however that this is not a serious issue, since the potential itself is not a physical observable, only the electric field is measurable. Since the electric field is obtained by taking the gradient of the scalar potential, it will be proportional to

$$V'(R) \sim \lambda \int_{-\infty}^{+\infty} \frac{dx}{(R^2 + x^2)^{3/2}}, \quad (\text{A.4})$$

which is perfectly convergent. It is however interesting to explore the possibility of providing a useful operative meaning to the definition of the scalar potential. To do that, we start by *regularizing* the integral in Eq. (A.3). This can be done by introducing the regularized $V_\Lambda(R)$ defined as

$$V_\Lambda(R) = \int_{-\Lambda}^{\Lambda} \lambda \frac{dx}{\sqrt{R^2 + x^2}} = \lambda \log \left[\frac{\sqrt{\Lambda^2 + R^2} + \Lambda}{\sqrt{\Lambda^2 + R^2} - \Lambda} \right]. \quad (\text{A.5})$$

We can then define the electric field as

$$\vec{E}(R) = \lim_{\Lambda \rightarrow \infty} [-\vec{\nabla} V_\Lambda(R)].$$

It is easy to check that this prescription leads to the right result:

$$\vec{E}(R) = \lim_{\Lambda \rightarrow \infty} \hat{R} \frac{2\lambda}{R} \frac{\Lambda}{\sqrt{\Lambda^2 + R^2}} \rightarrow \frac{2\lambda}{R} \hat{R}. \quad (\text{A.6})$$

Note that in this process we had to introduce a new variable Λ with the dimension of a length. This allows us to solve the puzzle first pointed out at the beginning. At the end, however, the dependence of the physical observable (i.e., the electric field) on this extra parameter disappears. Note also that the object,

$$\delta V = \lim_{\Lambda \rightarrow \infty} [V_\Lambda(r_2) - V_\Lambda(r_1)] = \lambda \log \left(\frac{r_1^2}{r_2^2} \right), \quad (\text{A.7})$$

is well defined. This suggests a way of defining the potential which is meaningful even in the $\Lambda \rightarrow \infty$ limit. We can *renormalize* the potential by subtracting $V(R)$ at some fixed value of $R = R_0$ and taking the $\Lambda \rightarrow \infty$ limit:

$$V(R) \rightarrow V(R) - V(R_0) = \lambda \log \left(\frac{R_0^2}{R^2} \right). \quad (\text{A.8})$$

The non-physical infinities present in $V(R)$ and $V(R_0)$ cancel each other, leaving a finite result, with a non-trivial R -dependence. Once again, this is possible because a dimensionful parameter (in this case R_0) has been introduced.

This example suggests a strategy for dealing with divergences.

- i) Identify an appropriate way to *regularize* infinite integrals.
- ii) Absorb the divergent terms into a redefinition of fields or parameters, e.g., via *subtractions*. This step is usually called *renormalization*.
- iii) Make sure the procedure is *consistent* by checking that the physical results do not depend on the regularization prescription.

In the rest of this appendix I will explain how this strategy is applied to the case of ultraviolet divergences encountered in perturbation theory.

A.2 Dimensional regularization

The typical expressions we have to deal with have the form

$$I(M^2) = \int \frac{d^4 \ell}{(2\pi)^4} \frac{1}{[\ell^2 + M^2]^2} . \quad (\text{A.9})$$

It is easy to show that the integral encountered in the quark self-energy diagram can be rewritten as

$$\frac{1}{\ell^2} \frac{1}{(\ell - p)^2} = \int_0^1 dx \frac{1}{(L^2 + M^2)^2}, \quad \text{with } L = \ell - xp, M^2 = x(1-x)p^2 . \quad (\text{A.10})$$

The most straightforward extension of the ideas presented above in the case of the infinite charged wire is to regularize the integral using a momentum cutoff, and to renormalize it with a subtraction [for example $I(M^2) - I(M_0^2)$]. Experience has shown, however, that the best way to regularize $I(M^2)$ is to take the analytic continuation of the integral in the number of space-time dimensions. In fact

$$I_D(M^2) = \int \frac{d^D \ell}{(2\pi)^D} \frac{1}{(\ell^2 + M^2)^2} \quad (\text{A.11})$$

is finite $\forall D < 4$. If we could assign a formal meaning to $I_D(M^2)$ for *continuous* values of D away from $D = 4$, we could then perform all our manipulations in $D \neq 4$, regulate the divergences, renormalize fields and couplings, and then go back to $D = 4$.

To proceed, one defines (for Euclidean metrics)

$$d^D \ell = d\Omega_{D-1} \ell^{D-1} d\ell \quad (\text{A.12})$$

with $d\Omega_{D-1}$ the differential solid angle in D dimensions. Ω_{D-1} is the surface of a D -dimensional sphere. It can be obtained by using the following formal identity:

$$\int d^D \ell e^{-\ell^2} \equiv \left[\int d\ell e^{-\ell^2} \right]^D = \pi^{D/2} . \quad (\text{A.13})$$

The integral can also be evaluated, using Eq. (A.12), as

$$\begin{aligned} \int d^D \ell e^{-\ell^2} &= \Omega_D \int_0^\infty \ell^{D-1} e^{-\ell^2} d\ell = \Omega_D \frac{1}{2} \int_0^\infty d\ell^2 (\ell^2)^{\frac{D-2}{2}} e^{-\ell^2} \\ &= \Omega_D \frac{1}{2} \int_0^\infty dx e^{-x} x^{\frac{D-2}{2}} \equiv \frac{\Omega_D}{2} \Gamma\left(\frac{D}{2}\right) . \end{aligned} \quad (\text{A.14})$$

Comparing Eqs. (A.13) and (A.14), we get

$$I_D(M^2) = \frac{1}{(4\pi)^{D/2}} \frac{1}{\Gamma(D/2)} \int_0^\infty dx x^{\frac{D-2}{2}} (x+M^2)^{-2} = \frac{1}{(4\pi)^{D/2}} \frac{\Gamma(2-D/2)}{\Gamma(2)} (M^2)^{\frac{D}{2}-2} . \quad (\text{A.15})$$

Defining $D = 4 - 2\epsilon$ (with the understanding that ϵ will be taken to 0 at the end of the day), and using the small- ϵ expansion,

$$\Gamma(\epsilon) = \frac{1}{\epsilon} - \gamma_\epsilon + \mathcal{O}(\epsilon) , \quad (\text{A.16})$$

we finally obtain

$$(4\pi)^2 I_D(M^2) \rightarrow \frac{1}{\epsilon} - \log 4\pi M^2 - \gamma_\epsilon . \quad (\text{A.17})$$

The divergent part of the integral is then regularized as a pole in $(D - 4)$. The M -dependent part of the integral behaves logarithmically, as expected because the integral itself was dimensionless in $D = 4$. The $1/\epsilon$ pole can be removed by a subtraction:

$$I(M^2) = I(\mu^2) + (4\pi)^2 \log\left(\frac{\mu^2}{M^2}\right) , \quad (\text{A.18})$$

where the subtraction scale μ^2 is usually referred to as the ‘renormalization scale’.

One can prove (and you will find this in the quoted textbooks) that other divergent integrals which appear in other loop diagrams can be regularized in a similar fashion, with the appearance of $1/\epsilon$ poles. Explicit calculations and more details on this technique can be found in the bibliography.

A.3 Renormalization

Let us come back now to our quark self-energy diagram, Eq. (A.1). After regulating the divergence using dimensional regularization, we can eliminate it by adding a counterterm to the Lagrangian:

$$\mathcal{L} \rightarrow \mathcal{L} + \Sigma(p)\bar{\psi}i\cancel{\partial}\psi = [1 + \Sigma(p)]\bar{\psi}i\cancel{\partial}\psi + \dots \quad (\text{A.19})$$

In this way, the corrections at $O(g^2)$ to the inverse propagator are finite:

$$\begin{array}{c} \text{---} \text{---} \text{---} \text{---} \text{---} \text{---} \\ \text{---} \text{---} \text{---} \text{---} \text{---} \text{---} \end{array} + \text{---} \text{---} \text{---} \text{---} \text{---} \text{---} \text{---} \text{---} \text{---} \text{---} \text{---} \text{---} = -i\cancel{p}\Sigma(p) + i\cancel{p}\Sigma(p) = 0. \quad (\text{A.20})$$

The inclusion of this counterterm can be interpreted as a renormalization of the quark wave function. To see this, it is sufficient to define

$$\psi_{\text{R}} = [1 + \Sigma(p^2)]^{1/2} \psi \quad (\text{A.21})$$

and verify that the kinetic part of the Lagrangian written in terms of ψ_{R} takes again the canonical form.

It may seem that this regularization/renormalization procedure can always be carried out, with all possible infinities being removed by *ad hoc* counter-terms. This is not true. That these subtractions can be performed consistently for any possible type of divergence which develops in perturbation theory is a highly non-trivial fact. To convince you of this, consider the following example.

Let us study the QCD corrections to the interaction of quarks with a photon:

$$\begin{array}{l} \begin{array}{c} \text{---} \text{---} \text{---} \text{---} \text{---} \text{---} \\ \text{---} \text{---} \text{---} \text{---} \text{---} \text{---} \end{array} \\ \begin{array}{l} \text{---} \text{---} \text{---} \text{---} \text{---} \text{---} \\ \text{---} \text{---} \text{---} \text{---} \text{---} \text{---} \end{array} \end{array} \quad \begin{aligned} &= (-ig)^2 C_{\text{F}} \int \frac{d^4\ell}{(2\pi)^4} \left[\gamma^p \frac{i}{\cancel{p} + \cancel{\ell}} \overbrace{(-ie\gamma^\mu)}^{\Gamma^\mu} \frac{i}{\cancel{p} + \cancel{\ell}} \gamma^p \right] \left(\frac{-i}{\ell^2} \right) \\ &= -ig^2 C_{\text{F}} \int \frac{d^4\ell}{(2\pi)^4} (-2)(\cancel{p} + \cancel{\ell})\Gamma^\mu(\cancel{p} + \cancel{\ell}) \frac{1}{\ell^2(p + \ell)^2(\bar{p} + \ell)^2} \\ &\xrightarrow{\text{leading div.}} -ig^2(-2)C_{\text{F}} \int \frac{d^4\ell}{(2\pi)^4} \frac{\cancel{\ell}\Gamma^\mu\cancel{\ell}}{\ell^2(p + \ell)^2(\bar{p} + \ell)^2} \stackrel{\text{def}}{=} ie\gamma^\mu V(q^2). \end{aligned}$$

It is easily recognized that $V(q^2)$ is divergent. The divergence can be removed by adding a counter-term to the bare Lagrangian:

$$\begin{aligned} \mathcal{L}_{\text{int}} &= -e A_\mu \bar{\psi} \gamma^\mu \psi \rightarrow -e A_\mu \bar{\psi} \gamma^\mu \psi - eV(q^2) A_\mu \bar{\psi} \gamma^\mu \psi \\ &= -[1 + V(q^2)] e A_\mu \bar{\psi} \gamma^\mu \psi. \end{aligned} \quad (\text{A.22})$$

If we take into account the counter-term that was introduced to renormalize the quark self-energy, the part of the quark Lagrangian describing the interaction with photons is now

$$\mathcal{L}_{q,\gamma} = [1 + \Sigma(p^2)] \bar{\psi} i \cancel{\partial} \psi - [1 + V(q^2)] e A_\mu \bar{\psi} \gamma^\mu \psi. \quad (\text{A.23})$$

Defining a renormalized charge by

$$e_{\text{R}} = e \frac{1 + V(p^2)}{1 + \Sigma(q^2)}, \quad (\text{A.24})$$

we are left with the renormalized Lagrangian

$$\mathcal{L}_R = \bar{\psi}_R i \not{\partial} \psi_R + e_R A_\mu \bar{\psi}_R \gamma^\mu \psi_R . \quad (\text{A.25})$$

Can we blindly accept this result, regardless of the values of the counter-terms $V(p^2)$ and $\Sigma(q^2)$? The answer to this question is NO! Charge conservation, in fact, requires $e_R = e$. The electric charge carried by a quark cannot be affected by the QCD corrections, and cannot be affected by the renormalization of QCD-induced divergences. There are many ways to see that if $e_R \neq e$ the electric charge would not be conserved in strong interactions. The simplest way is to consider the process $e^+ \nu_e \rightarrow W^+ \rightarrow u \bar{d}$. The electric charge of the initial state is +1 in units of e . After including QCD corrections (which in the case of the interaction with a W are the same as those for the interaction of quarks with a photon), the charge of the final state is +1 in units of e_R . Unless $e_R = e$, the total electric charge would not be conserved in this process! It is the non-renormalization of the electric charge in the presence of strong interactions that makes the charge of the proton equal to the sum of the charges of its constituent quarks, in spite of the complex QCD dynamics that holds the quarks together.

As a result, the renormalization procedure is consistent with charge conservation if and only if

$$\frac{V(q^2)}{\Sigma(p^2)} \stackrel{q^2 \rightarrow 0}{=} 1 . \quad (\text{A.26})$$

This identity should hold at all orders of perturbation theory. It represents a fundamental constraint on the consistency of the theory, and shows that the removal of infinities, by itself, is not a trivial trick which can be applied to arbitrary theories. Fortunately, the previous identity can be shown to hold. You can prove it explicitly at the one-loop order by explicitly evaluating the integrals defining $V(q)$ and $\Sigma(p)$.

To carry out the renormalization programme for QCD at one-loop order, several other diagrams in addition to the quark self-energy need to be evaluated. One needs the corrections to the gluon self-energy, to the coupling of a quark pair to a gluon, and to the three-gluon coupling. Each of these corrections gives rise to infinities, which can be regulated in dimensional regularization. For the purposes of renormalization, it is useful to apply the concept of D dimensions not only to the evaluation of the infinite integrals, but to the full theory as well. In other words, we should consider the Lagrangian as describing the interactions of fields in D dimensions. Nothing changes in its form, but the canonical dimensions of fields and couplings will be shifted. This is because the action (defined as the integral over space-time of the Lagrangian) is a dimensionless quantity. As a result, the canonical dimensions of the fields, and of the coupling constants, have to depend on D :

$$\begin{aligned} \left[\int d^D x \mathcal{L}(x) \right] &= 0 \Rightarrow [\mathcal{L}] = D = 4 - 2\epsilon , \\ [\partial_\mu \phi \partial^\mu \phi] &= D \Rightarrow [\phi] = 1 - \epsilon , \\ [\bar{\psi} \not{\partial} \psi] &= D \Rightarrow [\psi] = 3/2 - \epsilon , \\ [\bar{\psi} A \psi g] &= D \Rightarrow [g] = \epsilon . \end{aligned}$$

The gauge coupling constant acquires dimensions! This is a prelude to the non-trivial behaviour of the renormalized coupling constant as a function of the energy scale ("running"). But before we come to this, let us go back to the calculation of the counter-terms and the construction of the renormalized Lagrangian.

Replace the bare fields and couplings with renormalized ones:³

$$\begin{aligned} \psi_{\text{bare}} &= Z_2^{1/2} \psi_R , \\ A_{\text{bare}}^\mu &= Z_3^{1/2} A_R^\mu , \\ g_{\text{bare}} &= Z_g \mu^\epsilon g_R . \end{aligned}$$

³For the sake of simplicity, here and in the following we shall assume the quarks to be massless. The inclusion of the mass terms does not add any interesting new feature in what follows.

We explicitly extracted the dimensions out of g_{bare} , introducing the dimensional parameter μ (renormalization scale). In this way the renormalized coupling g_R is dimensionless (as it should be once we go back to four dimensions).

The Lagrangian, written in terms of renormalized quantities, becomes

$$\mathcal{L} = Z_2 \bar{\psi} i \not{\partial} \psi - \frac{1}{4} Z_3 F_{\mu\nu}^a F_a^{\mu\nu} + Z_g Z_2 Z_3^{1/2} \mu^\epsilon g \bar{\psi} \not{A} \psi + (\text{gauge fixing, ghosts, } \dots). \quad (\text{A.27})$$

It is customary to define

$$Z_1 = Z_g Z_2 Z_3^{1/2}. \quad (\text{A.28})$$

If we set $Z_n = 1 + \delta_n$, we then obtain

$$\begin{aligned} \mathcal{L} &= \bar{\psi} i \not{\partial} \psi - \frac{1}{4} F_{\mu\nu}^a F^{\mu\nu a} + \mu^\epsilon g \bar{\psi} \not{A} \psi + [\text{ghosts, gauge mixing}] \\ &+ \delta_2 \bar{\psi} i \not{\partial} \psi - \frac{1}{4} \delta_3 F_{\mu\nu}^a F^{\mu\nu a} + \delta_1 \mu^\epsilon g \bar{\psi} \not{A} \psi. \end{aligned} \quad (\text{A.29})$$

The counter-terms δ_i are fixed by requiring the one-loop Green functions to be finite. The explicit evaluation, which you can find carried out in detail, for example, in Refs. [3, 7], gives

$$\text{quark self-energy} \Rightarrow \delta_2 = -C_F \left(\frac{\alpha_s}{4\pi} \frac{1}{\epsilon} \right), \quad (\text{A.30})$$

$$\text{gluon self-energy} \Rightarrow \delta_3 = \left(\frac{5}{3} C_A - \frac{4}{3} n_F T_F \right) \frac{\alpha_s}{4\pi} \frac{1}{\epsilon}, \quad (\text{A.31})$$

$$q\bar{q}g \text{ vertex corrections} \Rightarrow \delta_1 = -(C_A + C_F) \frac{\alpha_s}{4\pi} \frac{1}{\epsilon}. \quad (\text{A.32})$$

As usual we introduced the notation $\alpha_s = g^2/4\pi$. The strong-coupling renormalization constant Z_g can be obtained using these results and Eq. (A.28):

$$Z_g = \frac{Z_1}{Z_2 Z_3^{1/2}} = 1 + \delta_1 - \delta_2 - \frac{1}{2} \delta_3 = 1 + \frac{\alpha_s}{4\pi} \frac{1}{\epsilon} \left[-\frac{11}{6} C_A + \frac{2}{3} n_F T_F \right] \stackrel{\text{def}}{=} 1 - \frac{1}{\epsilon} \left(\frac{b_0}{2} \right) \alpha_s. \quad (\text{A.33})$$

Note the cancellation of the terms proportional to C_F , between the quark self-energy (Z_2) and the Abelian part of the vertex correction (Z_1). This is the same as in the case of the QCD non-renormalization of the electric coupling, discussed at the beginning of this appendix. The non-Abelian part of the vertex correction contributes viceversa to the QCD coupling renormalization. This is a consequence of gauge invariance. The separation of the non-Abelian contributions to the self-energy and to the vertex is not gauge-invariant, only their sum is. Note also that the consistency of the renormalization procedure requires that the renormalized strong coupling g defining the strength of the interaction of quarks and gluons should be the same as that defining the interaction of gluons among themselves. If this did not happen, the gauge invariance of the $q\bar{q} \rightarrow gg$ process so painfully achieved in Section 2 by fixing the coefficient of the three-gluon coupling would no longer hold at one-loop! Once again, this additional constraint can be shown to hold through an explicit calculation.

A.4 Running of α_s

The running of α_s is a consequence of the renormalization-scale independence of the renormalization process. The bare coupling g_{bare} knows nothing about our choice of μ . The parameter μ is an artifact of the regularization prescription, introduced to define the dimensionful coupling in D dimensions, and should not enter in measurable quantities. As a result

$$\frac{dg_{\text{bare}}}{d\mu} = 0. \quad (\text{A.34})$$

Using the definition of g , $g_{\text{bare}} = \mu^\epsilon Z_g g$, we then get

$$\epsilon \mu^{2\epsilon} Z_g^2 \alpha_s + \mu^{2\epsilon} \alpha_s 2Z_g \frac{dZ_g}{dt} + \mu^{2\epsilon} Z_g^2 \frac{d\alpha_s}{dt} = 0 \quad (\text{A.35})$$

where

$$\frac{d}{dt} = \mu^2 \frac{d}{d\mu^2} = \frac{d}{d \log \mu^2} . \quad (\text{A.36})$$

Z_g depends upon μ only via the presence of α_s . If we define

$$\beta(\alpha_s) = \frac{d\alpha_s}{dt} , \quad (\text{A.37})$$

we then get

$$\beta(\alpha_s) + 2 \frac{\alpha_s}{Z_g} \frac{dZ_g}{d\alpha_s} \beta(\alpha_s) = -\epsilon \alpha_s . \quad (\text{A.38})$$

Using Eq. (A.33) and expanding in powers of α_s , we get

$$\beta(\alpha_s) = \frac{-\epsilon \alpha_s}{1 + 2 \frac{\alpha_s}{Z_g} \frac{dZ_g}{d\alpha_s}} = \frac{-\epsilon \alpha_s}{1 - \frac{b_0 \alpha_s}{\epsilon}} = -b_0 \alpha_s^2 + O(\alpha_s^2, \epsilon) \quad (\text{A.39})$$

and finally

$$\beta(\alpha_s) = -b_0 \alpha_s^2 \quad \text{with} \quad b_0 = \frac{1}{2\pi} \left(\frac{11}{6} C_A - \frac{2}{3} n_F T_F \right) \stackrel{N=3}{=} \frac{1}{12\pi} (33 - 2n_f) . \quad (\text{A.40})$$

We can now solve Eq. (A.37), assuming $b_0 > 0$ (which is true provided the number of quark flavours is less than 16) and get the famous *running* of α_s :

$$\alpha_s(\mu^2) = \frac{1}{b_0 \log(\mu^2/\Lambda^2)} . \quad (\text{A.41})$$

The parameter Λ describes the boundary condition of the first-order differential equation defining the running of α_s , and corresponds to the scale at which the coupling becomes infinity.

A.5 Renormalization group invariance

The fact that the coupling constant α_s depends on the unphysical renormalization scale μ should not be a source of worry. This is because the coupling constant itself is not an observable. What we observe are decay rates, spectra, or cross-sections. These are given by the product of the coupling constant and some matrix element, which in general will acquire a non-trivial renormalization-scale dependence through the renormalization procedure. We therefore just need to check that the scale dependence of the coupling constant and of the matrix elements cancel each other, leaving results which do not depend on μ .

Consider now a physical observable, for example the ratio $R = \sigma(e^+e^- \rightarrow \text{hadrons})/\sigma(e^+e^- \rightarrow \mu^+\mu^-)$. R can be calculated in perturbation theory within QCD, giving rise to an expansion in the renormalized coupling $\alpha_s(\mu)$:

$$R[\alpha_s, s/\mu^2] = 1 + \alpha_s f_1(t) + \alpha_s^2 f_2(t) + \dots = \sum_{n=0}^{\infty} \alpha_s^n f_{(n)}(t) , \quad (\text{A.42})$$

where $t = s/\mu^2$ (and we omitted a trivial overall factor $3 \sum_f Q_f^2$). R depends on μ explicitly via the functions $f_{(n)}(t)$ and implicitly through α_s . Since R is an observable, it should be independent of μ , and the functions $f_{(n)}(t)$ cannot be totally arbitrary. In particular, one should have

$$\mu^2 \frac{dR}{d\mu^2} = 0 = \left[\mu^2 \frac{\partial}{\partial \mu^2} + \beta(\alpha_s) \frac{\partial}{\partial \alpha_s} \right] R[\alpha_s, s/\mu^2] = 0 . \quad (\text{A.43})$$

Before we give the general, formal solution to this differential equation, it is instructive to work out directly its form within perturbation theory.

$$\mu^2 \frac{dR}{d\mu^2} = 0 = \beta(\alpha_s) f_1(t) + \alpha_s \mu^2 \frac{df_1}{d\mu^2} + 2\alpha_s \beta(\alpha_s) f_2(t) + \alpha_s^2 \mu^2 \frac{df_2}{d\mu^2} + \dots \quad (\text{A.44})$$

At order α_s (remember that β is of order α_s^2) we get

$$\frac{df_1}{d\mu^2} = 0 \Rightarrow f_1 = \text{constant} \equiv a_1. \quad (\text{A.45})$$

This is by itself a non-trivial result! It says that the evaluation of R at one-loop is finite, all UV infinities must cancel without charge renormalization. If they did not cancel, f_1 would depend explicitly on μ . As we saw at the beginning, this is a consequence of the non-renormalization of the electric charge.

At order α_s^2 we have

$$\beta(\alpha_s) f_1(t) + \alpha_s^2 \frac{df_2}{d \log \mu^2} = 0 \Rightarrow f_2 = b_0 a_1 \log \frac{\mu^2}{s} + a_2 \text{ (integration constant)}. \quad (\text{A.46})$$

So up to order α_s^2 we have

$$R = 1 + \underbrace{a_1 \alpha_s}_{\text{one-loop}} + \underbrace{a_1 b_0 \alpha_s^2 \log \mu^2/s + a_2 \alpha_s^2}_{\text{two-loops}} + \dots \quad (\text{A.47})$$

Note that the requirement of renormalization group invariance allows us to know the coefficient of the logarithmic term at two loops without having to carry out the explicit two-loop calculation! It is also important to notice that in the limit of high energy, $s \rightarrow \infty$, the logarithmic term of the two-loop contribution becomes very large, and this piece becomes numerically of order α_s as soon as $\log s/\mu^2 \gtrsim 1/b_0 \alpha_s$. It is easy to check that renormalization scale invariance requires the presence of such logs at all orders of perturbation theory. In particular,

$$f_{(n)}(t) = a_1 \left[b_0 \log \frac{\mu^2}{s} \right]^n + \dots \quad (\text{A.48})$$

We can collect all these logs as follows:

$$R = 1 + a_1 \alpha_s \left[1 + \alpha_s b_0 \log \frac{\mu^2}{s} + (\alpha_s b_0 \log \frac{\mu^2}{s})^2 + \dots \right] + a_2 \alpha_s^2 + \dots \quad (\text{A.49})$$

$$= 1 + a_1 \frac{\alpha_s(\mu)}{1 + \alpha_s(\mu) b_0 \log \frac{s}{\mu^2}} + a_2 \alpha_s^2 + \dots \equiv 1 + a_1 \alpha_s(s) + a_2 \alpha_s^2 + \dots \quad (\text{A.50})$$

In fact,

$$\frac{\alpha_s(\mu)}{1 + \alpha_s(\mu) b_0 \log \frac{s}{\mu^2}} = \frac{1}{b_0 \log \frac{\mu^2}{\Lambda^2} + b_0 \log \frac{s}{\mu^2}} = \frac{1}{b_0 \log \frac{s}{\Lambda^2}} \equiv \alpha_s(s). \quad (\text{A.51})$$

Renormalization group invariance constrains the form of higher-order corrections. All of the higher-order logarithmic terms are determined in terms of lower-order finite coefficients. They can be resummed by simply setting the scale of α_s to s . You can check by yourself that this will work also for the higher-order terms, such as those proportional to a_2 . So the final result has the form

$$R = 1 + a_1 \alpha_s(s) + a_2 \alpha_s^2(s) + a_3 \alpha_s^3(s) + \dots \quad (\text{A.52})$$

Of course a_1, a_2, \dots have to be determined by an explicit calculation. However, the truncation of the series at order n has now an accuracy which is truly of order α_s^{n+1} , contrary to before when higher-order terms were as large as lower-order ones. The explicit calculation has been carried out up to the a_3 coefficient. In particular,

$$a_1 = \frac{3}{4} \frac{C_F}{\pi} \equiv \frac{1}{\pi}. \quad (\text{A.53})$$

The formal proof of the previous equation can be obtained by showing that the general form of the equation

$$\left[\mu^2 \frac{\partial}{\partial \mu^2} + \beta(\alpha_s) \right] R(\alpha_s, \frac{s}{\mu^2}) = 0 \quad (\text{A.54})$$

is given by

$$\begin{cases} R(\alpha_s(s), 1), & \text{with} \\ \frac{d\alpha_s}{d \log \frac{s}{\mu^2}} = \beta(\alpha_s) \end{cases} . \quad (\text{A.55})$$

B Formal derivation of the evolution equations

Assuming the parton picture outlined above, we can describe the cross-section for the interaction of the virtual photon with the proton as follows:

$$\sigma_0 = \int_0^1 dx \sum_i e_i^2 f_i(x) \hat{\sigma}_0(\gamma^* q_i \rightarrow q'_i, x) \quad (\text{B.1})$$

where the 0 subscript anticipates that this description represents a leading order approximation. In the above equation, $f_i(x)$ represents the density of quarks of flavour i carrying a fraction x of the proton momentum. The hatted cross-section represents the interaction between the photon and a free (massless) quark:

$$\begin{aligned} \hat{\sigma}_0(\gamma^* q_i \rightarrow q'_i) &= \frac{1}{\text{flux}} \overline{\sum} |M_0(\gamma^* q \rightarrow q')|^2 \frac{d^3 p'}{(2\pi)^3 2p'_0} (2\pi)^4 \delta^4(p' - q - p) \\ &= \frac{1}{\text{flux}} \overline{\sum} |M_0|^2 2\pi \delta(p'^2) . \end{aligned} \quad (\text{B.2})$$

Using $p' = xP + q$, where P is the proton momentum, we get

$$(p')^2 = 2xP \cdot q + q^2 \equiv 2xP \cdot q - Q^2, \quad (\text{B.3})$$

$$\hat{\sigma}_0(\gamma^* q \rightarrow q') = \frac{2\pi}{\text{flux}} \overline{\sum} |M_0|^2 \frac{1}{2P \cdot q} \delta(x - x_{bj}), \quad (\text{B.4})$$

where $x_{bj} = \frac{Q^2}{2P \cdot q}$ is the so-called Bjorken- x variable. Finally,

$$\sigma_0 = \frac{2\pi}{\text{flux}} \frac{\overline{\sum} |M_0|^2}{Q^2} \sum_i x_{bj} f_i(x_{bj}) e_i^2 \equiv \frac{2\pi}{\text{flux}} \frac{\overline{\sum} |M_0|^2}{Q^2} F_2(x_{bj}). \quad (\text{B.5})$$

The measurement of the inclusive ep cross-section as a function of Q^2 and $P \cdot q [= m_p(E' - E)]$ in the proton rest frame, with E' = energy of final-state lepton and E = energy of initial-state lepton] probes the quark momentum distribution inside the proton.

B.1 Parton evolution

Let us now study the QCD corrections to the LO parton-model description of DIS. This study will exhibit many important aspects of QCD (structure of collinear singularities, renormalization-group invariance) and will take us to an important element of the DIS phenomenology, namely scaling violations. We start from real-emission corrections to the Born level process:

$$\text{Diagram 1} + \text{Diagram 2} \quad (\text{B.6})$$

The first diagram is proportional to $1/(p-k)^2 = 1/2(pk)$, which diverges when k is emitted parallel to p :

$$p \cdot k = p^0 k^0 (1 - \cos \theta) \xrightarrow{\cos \theta \rightarrow 1} 0. \quad (\text{B.7})$$

The second diagram is also divergent, if k is emitted parallel to p' . This second divergence turns out to be harmless, since we are summing over all possible final states. Whether the final-state quark keeps all of its energy, or whether it decides to share it with a gluon emitted collinearly, an inclusive final-state measurement will not care. The collinear divergence can then be cancelled by a similar divergence appearing in the final-state quark self-energy corrections.

The first divergence is more serious, since from the point of view of the incoming photon (which only sees the quark, not the gluon) it *does* make a difference whether the momentum is all carried by the quark or is shared between the quark and the gluon. This means that no cancellation between collinear singularities in the real emission and virtual emission is possible. So let us go ahead, calculate explicitly the contribution of these diagrams, and learn how to deal with their singularities.

First of all, note that while the second diagram is not singular in the region $k \cdot p \rightarrow 0$, its interference with the first one is. It is possible, however, to select a gauge for which the interference of the two diagrams is finite in this limit. It can be shown that the right choice is

$$\sum \epsilon_\mu \epsilon_\nu^*(k) = -g_{\mu\nu} + \frac{k^\mu p'^\nu + k^\nu p'^\mu}{k \cdot p'}. \quad (\text{B.8})$$

Note that in this gauge not only $k \cdot \epsilon(k) = 0$, but also $p' \cdot \epsilon(k) = 0$. The key to getting to the end of a QCD calculation in a finite amount of time is choosing a proper gauge (which we just did) and the proper parametrization of the momenta involved. In our case, since we are interested in isolating the region where k becomes parallel with p , it is useful to set

$$k_\mu = (1-z)p_\mu + \beta p'_\mu + (k_\perp)_\mu, \quad (\text{B.9})$$

with $k_\perp \cdot p = k_\perp \cdot p' = 0$. β is obtained by imposing

$$k^2 = 0 = 2\beta(1-z)p \cdot p' + k_\perp^2. \quad (\text{B.10})$$

Defining $k_\perp^2 = -k_t^2$, we then get

$$\beta = \frac{k_t^2}{2(pp')(1-z)}, \quad (\text{B.11})$$

$$k_\mu = (1-x)p_\mu + \frac{k_t^2}{2(1-x)p \cdot p'} p'_\mu + (k_\perp)_\mu. \quad (\text{B.12})$$

$(k_\perp)_\mu$ is therefore the gluon momentum vector transverse to the incoming quark, in a frame where γ^* and q are aligned. k_t is the value of this transverse momentum. We also get

$$k \cdot p = \beta p \cdot p' = \frac{k_t^2}{2(1-z)} \quad \text{and} \quad k \cdot p' = (1-z)p \cdot p'. \quad (\text{B.13})$$

As a result $(p-k)^2 = -k_t^2/(1-z)$. The amplitude for the only diagram carrying the initial-state singularity is

$$M_g = ig\lambda_{ij}^a \bar{u}(p') \Gamma \frac{\hat{p} - \hat{k}}{(p-k)^2} \hat{\epsilon}(k) u(p) \quad (\text{B.14})$$

(where we introduced the notation $\hat{a} \equiv \not{a} \equiv a_\mu \gamma^\mu$). We indicated by Γ the interaction vertex with the external current q . It is important to keep Γ arbitrary, because we would like to get results which do not depend on the details of the interaction with the external probe. It is important that the singular part of the QCD correction, and therefore its renormalization, be process independent. Only in this way can we

hope to achieve a true universality of the parton densities! So we will keep Γ generic, and make sure that our algebra does not depend on its form, at least in the $p \cdot k \rightarrow 0$ limit. Squaring the most singular part of the amplitude, and summing over colours and spins, we get

$$\sum_{\substack{\text{g polariz.} \\ \text{and colours}}} |M_g|^2 = g^2 \sum_a \overbrace{\text{tr}(\lambda^a \lambda^a)}^{N \times C_F} \times \frac{1}{t^2} \times \sum_{\epsilon} \text{tr}[\hat{p}' \Gamma (\hat{p} - \hat{k}) \hat{\epsilon} \cdot p \hat{\epsilon}^* (\hat{p} - \hat{k}) \Gamma^+] \quad (\text{B.15})$$

with $t = (p - k)^2 = -k_t^2/(1 - z)$. Let us look first at

$$\sum_{\epsilon} \hat{\epsilon} \hat{p} \hat{\epsilon}^* = \sum_{\epsilon} \epsilon_{\mu} \epsilon_{\nu}^* \gamma^{\mu} \hat{p} \gamma^{\nu} = -\gamma^{\mu} \hat{p} \gamma^{\mu} + \frac{1}{k \cdot p'} (\hat{p}' \hat{p} \hat{k} + \hat{k} \hat{p} \hat{p}') = \frac{2}{1 - z} (\hat{k} + \beta \hat{p}') \quad (\text{B.16})$$

(we used $\hat{a} \hat{b} \hat{c} + \hat{c} \hat{b} \hat{a} = 2(a \cdot b) \hat{c} - 2(a \cdot c) \hat{b} + 2(b \cdot c) \hat{a}$ and some of the kinematical relations from the previous page). Then take

$$(\hat{p} - \hat{k}) (\hat{k} + \beta \hat{p}') (\hat{p} - \hat{k}) = (\hat{p} - \hat{k}) \hat{k} (\hat{p} - \hat{k}) + \beta (\hat{p} - \hat{k}) \hat{p}' (\hat{p} - \hat{k}). \quad (\text{B.17})$$

In the second term, proportional to β , we can approximate $\hat{k} = (1 - z)\hat{p}$. This is because the other pieces ($\beta \hat{p}' + \hat{k}_{\perp}$) multiplied by β would cancel entirely the $\frac{1}{t^2}$ singularity, and would only contribute a non-singular term, which we are currently neglecting. So Eq. (B.17) becomes

$$\hat{p} \hat{k} \hat{p} + \beta z^2 \hat{p} \hat{p}' \hat{p} = 2(p \cdot k) \hat{p} + \beta z^2 2(p \cdot p') \hat{p} = 2(p \cdot k) (1 + z^2) \hat{p} \quad (\text{B.18})$$

and

$$\sum |M_g|^2 = 2g^2 C_F \frac{(1 - z)}{k_t^2} \left(\frac{1 + z^2}{1 - z} \right) N \text{tr}[\hat{p}' \Gamma \hat{p} \Gamma^+]. \quad (\text{B.19})$$

The last factor with the trace corresponds to the Born amplitude squared. So the one-gluon emission process factorizes in the collinear limit into the Born process times a factor which is independent of the beam's nature! If we add the gluon phase-space

$$[dk] \equiv \frac{d^3 k}{(2\pi)^3 2k^0} = \frac{dk_{\parallel}}{k^0} \frac{d\phi}{2\pi} \frac{1}{8\pi^2} \frac{dk_{\perp}^2}{2} = \frac{dz}{(1 - z)} \frac{1}{16\pi^2} dk_{\perp}^2, \quad (\text{B.20})$$

we get

$$\overline{\sum} |M_g|^2 [dk] = \frac{dk_{\perp}^2}{k_{\perp}^2} dz \left(\frac{\alpha_s}{2\pi} \right) P_{qq}(z) \overline{\sum} |M_0|^2 \quad (\text{B.21})$$

where

$$P_{qq}(z) = C_F \frac{1 + z^2}{1 - z} \quad (\text{B.22})$$

is the so-called Altarelli–Parisi splitting function for the $q \rightarrow q$ transition (z is the momentum fraction of the original quark taken away by the quark after gluon emission). We are now ready to calculate the corrections to the parton-model cross-section:

$$\sigma_g = \int dx f(x) \frac{1}{\text{flux}} \int dz \frac{dk_{\perp}^2}{k_{\perp}^2} \left(\frac{\alpha_s}{2\pi} \right) P_{qq}(z) \overline{\sum} |M_0|^2 2\pi \delta(p'^2). \quad (\text{B.23})$$

Using $(p')^2 = (p - k + q)^2 \sim (zp + q)^2 = (xzP + q)^2$ and

$$\delta(p'^2) = \frac{1}{2P \cdot q} \frac{1}{z} \delta(x - \frac{x_{bj}}{z}) = \frac{x_{bj}}{z} \delta(x - \frac{x_{bj}}{z}), \quad (\text{B.24})$$

we finally obtain

$$\sigma_g = \frac{2\pi}{\text{flux}} \left(\frac{\sum_i |M_0|^2}{Q^2} \right) \sum_i e_i^2 x_{bj} \frac{\alpha_s}{2\pi} \int \frac{dk_\perp^2}{k_\perp^2} \int \frac{dz}{z} P_{qq}(z) f_i \left(\frac{x_{bj}}{z} \right). \quad (\text{B.25})$$

We then find that the inclusion of the $\mathcal{O}(\alpha_s)$ correction is equivalent to a contribution to the parton density:

$$f_i(x) \rightarrow f_i(x) + \frac{\alpha_s}{2\pi} \int \frac{dk_\perp^2}{k_\perp^2} \int_x^1 \frac{dz}{z} P_{qq}(z) f_i \left(\frac{x}{z} \right). \quad (\text{B.26})$$

Note the presence of the integral $\int dk_\perp^2/k_\perp^2$. The upper limit of integration is proportional to Q^2 . The lower limit is 0. Had we included a quark mass, the propagator would have behaved like $1/(k_\perp^2 + m^2)$. But the quark is bound inside the hadron, so we do not quite know what m should be. Let us then assume that we cut off the integral at a k_\perp value equal to some scale μ_0 , and see what happens. The effective parton density becomes

$$f(x, Q^2) = f(x) + \log \left(\frac{Q^2}{\mu_0^2} \right) \frac{\alpha_s}{2\pi} \int_x^1 \frac{dz}{z} P_{qq}(z) f \left(\frac{x}{z} \right). \quad (\text{B.27})$$

The dependence on the scale μ_0 , which is a non-perturbative scale, can be removed by defining $f(x, Q^2)$ in terms of the parton density f measured at a large, perturbative scale μ^2 :

$$f(x, \mu^2) = f(x) + \log \left(\frac{\mu^2}{\mu_0^2} \right) \frac{\alpha_s}{2\pi} \int_x^1 \frac{dz}{z} P_{qq}(z) f \left(\frac{x}{z} \right). \quad (\text{B.28})$$

We can then perform a subtraction, and write

$$f(x, Q^2) = f(x, \mu^2) + \log \left(\frac{Q^2}{\mu^2} \right) \frac{\alpha_s}{2\pi} \int_x^1 \frac{dz}{z} P_{qq}(z) f \left(\frac{x}{z} \right). \quad (\text{B.29})$$

The scale μ plays here a similar role to the renormalization scale introduced in the Appendix A. Its choice is arbitrary, and $f(x, Q^2)$ should not depend on it. Requiring this independence, we get the following ‘renormalization-group (RG) invariance’ condition:

$$\frac{df(x, Q^2)}{d \ln \mu^2} = \mu^2 \frac{df(x, \mu^2)}{d\mu^2} - \frac{\alpha_s}{2\pi} \int_x^1 \frac{dz}{z} P_{qq}(z) f \left(\frac{x}{z} \right) \equiv 0 \quad (\text{B.30})$$

and then

$$\mu^2 \frac{df(x, \mu^2)}{d\mu^2} = \frac{\alpha_s}{2\pi} \int_x^1 \frac{dz}{z} P_{qq}(z) f \left(\frac{x}{z}, \mu^2 \right). \quad (\text{B.31})$$

This equation is usually called the DGLAP (Dokshitzer–Gribov–Lipatov–Altarelli–Parisi) equation. As in the case of the resummation of leading logarithms in $R_{e^+e^-}$ induced by the RG invariance constraints, the DGLAP equation—which is the result of RG invariance—resums a full tower of leading logarithms of Q^2 .

Proof: Let us define $t = \log \frac{Q^2}{\mu^2}$. We can then expand $f(x, t)$ in powers of t :

$$f(x, t) = f(x, 0) + t \frac{df}{dt}(x, 0) + \frac{t^2}{2!} \frac{d^2 f}{dt^2}(x, 0) + \dots \quad (\text{B.32})$$

The first derivative is given by the DGLAP equation itself. Higher derivatives can be obtained by differentiating it:

$$f''(x, t) = \frac{\alpha_s}{2\pi} \int \frac{dz}{z} P_{qq}(z) \frac{df}{dt} \left(\frac{x}{z}, t \right)$$

$$\begin{aligned}
&= \frac{\alpha_s}{2\pi} \int_x^1 \frac{dz}{z} P_{qq}(z) \frac{\alpha_s}{2\pi} \int_{\frac{x}{z}}^1 \frac{dz'}{z'} P_{qq}(z) f\left(\frac{x}{zz'}, t\right) \\
&\vdots \\
f^{(h)}(x, t) &= \frac{\alpha_s}{2\pi} \int_x^1 \dots \frac{\alpha_s}{2\pi} \int_{x/zz' \dots z^{(n-1)}}^1 \frac{dz^{(n)}}{z^{(n)}} P_{qq}(z^{(n)}) f\left(\frac{x}{zz' \dots z^{(n)}}, t\right). \quad (\text{B.33})
\end{aligned}$$

The n -th term in this expansion, proportional to $(\alpha_s t)^n$, corresponds to the emission of n gluons (it is just the n -fold iteration of what we did studying the one-gluon emission case).

With similar calculations one can include the effect of the other $\mathcal{O}(\alpha_s)$ correction, originating from the splitting into a $q\bar{q}$ pair of a gluon contained in the proton. With the addition of this term, the evolution equation for the density of the i th quark flavour becomes

$$\frac{df_q(x, t)}{dt} = \frac{\alpha_s}{2\pi} \int_x^1 \frac{dz}{z} \left[P_{qq}(z) f_i\left(\frac{x}{z}, t\right) + P_{qg}(z) f_g\left(\frac{x}{z}, t\right) \right], \quad \text{with } P_{qg} = \frac{1}{2} [z^2 + (1-z)^2]. \quad (\text{B.34})$$

In the case of interactions with a coloured probe (say a gluon) we meet the following corrections, which affect the evolution of the gluon density $f_g(x)$:

$$\frac{df_g(x, t)}{dt} = \frac{\alpha_s}{2\pi} \int_x^1 \frac{dz}{z} \left[P_{gq}(z) \sum_{i=q, \bar{q}} f_i\left(\frac{x}{z}, t\right) + P_{gg}(z) f_g\left(\frac{x}{z}, t\right) \right] \quad (\text{B.35})$$

with

$$P_{qg}(z) = P_{gq}(1-z) = C_F \frac{1 + (1-z)^2}{z} \quad \text{and} \quad P_{gg}(z) = 2C_A \left[\frac{1-z}{z} + \frac{z}{1-z} + z(1-z) \right]. \quad (\text{B.36})$$

Defining the moments of an arbitrary function $g(x)$ as follows,

$$g_n = \int_0^1 \frac{dx}{x} x^n g(x),$$

it is easy to prove that the evolution equations turn into ordinary linear differential equations:

$$\frac{df_i^{(n)}}{dt} = \frac{\alpha_s}{2\pi} [P_{qq}^{(n)} f_i^{(n)} + P_{qg}^{(n)} f_g^{(n)}], \quad (\text{B.37})$$

$$\frac{df_g^{(n)}}{dt} = \frac{\alpha_s}{2\pi} [P_{gg}^{(n)} f_g^{(n)} + P_{gq}^{(n)} f_i^{(n)}]. \quad (\text{B.38})$$

B.2 Properties of the evolution equations

We now study some general properties of these equations. It is convenient to introduce the concepts of *valence* $[V(x, t)]$ and *singlet* $[\Sigma(x, t)]$ densities:

$$V(x) = \sum_i f_i(x) - \sum_{\bar{i}} f_{\bar{i}}(x), \quad (\text{B.39})$$

$$\Sigma(x) = \sum_i f_i(x) + \sum_{\bar{i}} f_{\bar{i}}(x), \quad (\text{B.40})$$

where the index \bar{i} refers to the antiquark flavours. The evolution equations then become

$$\frac{dV^{(n)}}{dt} = \frac{\alpha_s}{2\pi} P_{qq}^{(n)} V^{(n)}, \quad (\text{B.41})$$

$$\frac{d\Sigma^{(n)}}{dt} = \frac{\alpha_s}{2\pi} \left[P_{qq}^{(n)} \Sigma^{(n)} + 2n_f P_{qg}^{(n)} f_g^{(n)} \right], \quad (\text{B.42})$$

$$\frac{df_g^{(n)}}{dt} = \frac{\alpha_s}{2\pi} \left[P_{gq}^{(n)} \Sigma^{(n)} + P_{gg}^{(n)} f_g^{(n)} \right]. \quad (\text{B.43})$$

Note that the equation for the valence density decouples from the evolution of the gluon and singlet densities, which are coupled among themselves. This is physically very reasonable, since in perturbation theory the contribution to the quark and the antiquark densities coming from the evolution of gluons (via their splitting into $q\bar{q}$ pairs) is the same, and will cancel out in the definition of the valence. The valence therefore only evolves because of gluon emission. On the contrary, gluons and $q\bar{q}$ pairs in the proton *sea* evolve into one another.

The first moment of $V(x)$, $V^{(1)} = \int_0^1 dx V(x)$, counts the number of valence quarks. We therefore expect it to be independent of Q^2 :

$$\frac{dV^{(1)}}{dt} \equiv 0 = \frac{\alpha_s}{2\pi} P_{qq}^{(1)} V^{(1)} = 0. \quad (\text{B.44})$$

Since $V^{(1)}$ itself is different from 0, we obtain a constraint on the first moment of the splitting function: $P_{qq}^{(1)} = 0$. This constraint is satisfied by including the effect of the virtual corrections, which generate a contribution to $P_{qq}(z)$ proportional to $\delta(1-z)$. This correction is incorporated in $P_{qq}(z)$ via the redefinition:

$$P_{qq}(z) \rightarrow \left(\frac{1+z^2}{1-z} \right)_+ \equiv \frac{1+z^2}{1-z} - \delta(1-z) \int_0^1 dy \left(\frac{1+y^2}{1-y} \right) \quad (\text{B.45})$$

where the + sign turns $P_{qq}(z)$ into a distribution. In this way, $\int_0^1 dz P_{qq}(z) = 0$ and the valence sum-rule is obeyed at all Q^2 .

Another sum-rule that does not depend on Q^2 is the momentum sum-rule, which imposes the constraint that all of the momentum of the proton is carried by its constituents (valence plus sea plus gluons):

$$\int_0^1 dx x \left[\sum_{i,\bar{i}} f_i(x) + f_g(x) \right] \equiv \Sigma^{(2)} + f_g^{(2)} = 1. \quad (\text{B.46})$$

Once more this relation should hold for all Q^2 values, and this can be proved by using the evolution equations that this implies:

$$P_{qq}^{(2)} + P_{gq}^{(2)} = 0, \quad (\text{B.47})$$

$$P_{gg}^{(2)} + 2n_f P_{qg}^{(2)} = 0. \quad (\text{B.48})$$

You can check using the definition of second moment, and the explicit expressions of the P_{qq} and P_{gq} splitting functions, that the first condition is automatically satisfied. The second condition is satisfied by including the virtual effects in the gluon propagator, which contribute a term proportional to $\delta(1-z)$. It is a simple exercise to verify that the final form of the $P_{gg}(z)$ splitting function, satisfying Eq. (B.48), is

$$P_{gg} \rightarrow 2C_A \left\{ \frac{x}{(1-x)_+} + \frac{1-x}{x} + x(1-x) \right\} + \delta(1-x) \left[\frac{11C_A - 2n_f}{6} \right]. \quad (\text{B.49})$$

B.3 Solution of the evolution equations

The evolution equations formulated in the previous section can be solved analytically in moment space. The boundary conditions are given by the moments of the parton densities at a given scale μ , where in principle they can be obtained from a direct measurement. The solution at different values of the scale Q can then be obtained by inverting numerically the expression for the moments back to x space. The

resulting evolved densities can then be used to calculate cross-sections for an arbitrary process involving hadrons, at an arbitrary scale Q . We shall limit ourselves here to studying some properties of the analytic solutions, and will present and comment on some plots obtained from numerical studies available in the literature.

As an exercise, you can show that the solution of the evolution equation for the valence density is the following:

$$V^{(n)}(Q^2) = V^{(n)}(\mu^2) \left[\frac{\log Q^2/\Lambda^2}{\log \mu^2/\Lambda^2} \right]^{P_{qq}^{(n)}/2\pi b_0} = V^{(n)}(\mu^2) \left[\frac{\alpha_s(\mu^2)}{\alpha_s(Q^2)} \right]^{P_{qq}^{(n)}/2\pi b_0} \quad (\text{B.50})$$

where the running of $\alpha_s(\mu^2)$ has to be taken into account to get the right result. Since all moments $P^{(n)}$ are negative, the evolution to larger values of Q makes the valence distribution softer and softer. This is physically reasonable, since the only thing that the valence quarks can do is to lose energy because of gluon emission.

The solutions for the gluon and singlet distributions f_g and Σ can be obtained by diagonalizing the 2×2 system in Eqs. (B.42) and (B.43). We study the case of the second moments, which correspond to the momentum fractions carried by quarks and gluons separately. In the asymptotic limit $\Sigma^{(2)}$ goes to a constant, and $\frac{d\Sigma^{(2)}}{dt} = 0$. Then, using the momentum sum-rule,

$$P_{qq}^{(2)} \Sigma^{(2)} + 2n_f P_{qq}^{(2)} f_g^{(2)} = 0, \quad (\text{B.51})$$

$$\Sigma^{(2)} + f_g^{(2)} = 1. \quad (\text{B.52})$$

The solution of this system is

$$\Sigma^{(2)} = \frac{1}{1 + \frac{4C_F}{n_f}} \quad (= 15/31 \text{ for } n_f = 5), \quad (\text{B.53})$$

$$f_g^{(2)} = \frac{4C_F}{4C_F + n_f} \quad (= 16/31 \text{ for } n_f = 5). \quad (\text{B.54})$$

As a result, the fraction of momentum carried by gluons is asymptotically approximately 50% of the total proton momentum. It is interesting to note that, experimentally, this asymptotic value is actually reached already at rather low values of Q^2 . It was indeed observed already since the early days of the DIS experiments that only approximately 50% of the proton momentum was carried by charged constituents. This was one of the early pieces of evidence for the existence of gluons.

A complete solution for the evolved parton densities in x space can only be obtained from a numerical analysis. This work has been done in the past by several groups (see e.g., the discussions in Ref. [8]), and is continuously being updated by including the most up-to-date experimental results used for the determination of the input densities at a fixed scale.

C Jet rates in e^+e^- collisions

We present here explicit calculations of a few interesting jet observables in e^+e^- collisions. For simplicity, we will work with the soft-gluon approximation for the matrix elements and the phase-space. As a result, the correction to the differential $e^+e^- \rightarrow q\bar{q}$ cross-section from one-gluon emission becomes

$$d\sigma_g = \sigma_0 \frac{2\alpha_s}{\pi} C_F \frac{dk_0}{k_0} \frac{d\cos\theta}{1 - \cos^2\theta}, \quad \text{where } \sigma_0 \text{ is the Born amplitude.} \quad (\text{C.1})$$

In this equation we used the fact that in the soft- g limit the q and \bar{q} are back-to-back, and

$$q \cdot \bar{q} = 2q_0\bar{q}_0, \quad q \cdot k = q_0k_0(1 - \cos\theta), \quad \bar{q} \cdot k = \bar{q}_0k_0(1 + \cos\theta). \quad (\text{C.2})$$

Note the presence in $d\sigma_g$ of soft and collinear singularities. They will have to cancel in the total cross-section which, as we saw in the previous lecture, is finite. They do indeed cancel against the contribution to the total cross-section coming from the virtual correction diagram, where a gluon is exchanged between the two quarks. In the total cross-section (and for other sufficiently inclusive observables) the final states produced by the virtual diagrams and by the real emission diagrams in the soft or collinear limit are the same, and both contribute. In order for the total cross-section to be finite, the virtual contribution will need to take the following form:

$$\frac{d^2\sigma_v}{dk_0 d\cos\theta} = -\sigma_0 \frac{2\alpha_s}{\pi} C_F \int_0^{\sqrt{s/2}} \frac{dk'_0}{k'_0} \int_{-1}^1 \frac{d\cos\theta'}{1-\cos^2\theta'} \times \frac{1}{2} \delta(k_0) [\delta(1-\cos\theta) + \delta(1+\cos\theta)] \quad (\text{C.3})$$

plus finite corrections. In this way,

$$\int_0^{\sqrt{s/2}} dk_0 \int_{-1}^1 d\cos\theta \left[\frac{d^2\sigma_g}{dk_0 d\cos\theta} + \frac{d^2\sigma_v}{dk_0 d\cos\theta} \right] = \text{finite} . \quad (\text{C.4})$$

With the form of the virtual corrections available (at least in this simplified soft-gluon-dominated approximation), we can proceed and calculate other quantities.

Jets are usually defined as clusters of particles close-by in phase-space. A typical jet definition distributes particles in sets of invariant mass smaller than a given parameter M , requiring that one particle only belongs to one jet, and that no other particles (or jets) can be added to a given jet without its mass exceeding M . In the case of a three-particle final state, such as the one we are studying, we get three-jet events if $(q+k)^2$, $(\bar{q}+k)^2$ and $(q+\bar{q})^2$ are all larger than M^2 . We will have two-jet events when at least one of these quantities gets smaller than M^2 . For example emission of a gluon near the direction of the quark, with $2qk = 2q^0k^0(1-\cos\theta) < M^2$, defines a two-jet event, one jet being given by the \bar{q} , the other by the system $q+k$.

One usually introduces the parameter $y = M^2/s$, and studies the jet multiplicity as a function of y . Let us calculate the two- and three-jet rates at order α_s . The phase-space domain for two-jet events is given by two regions. The first one is defined by $2qk = 2q_0k_0(1-\cos\theta) < ys$. This region consists of two parts:

$$(I)_a : \left\{ \begin{array}{l} k_0 < y\sqrt{s} \\ 0 < \cos\theta < 1 \end{array} \right. \quad \oplus \quad (I)_b : \left\{ \begin{array}{l} k_0 > y\sqrt{s} \\ 1 - \frac{y\sqrt{s}}{k_0} < \cos\theta < 1 \end{array} \right. . \quad (\text{C.5})$$

$(I)_a$ corresponds to soft gluons at all angles smaller than $\pi/2$ (i.e., in the quark emisphere), and $(I)_b$ corresponds to hard gluons emitted at small angles from the quark.

The second region, (II) , is analogous to (I) , but the angles are now referred to the direction of the antiquark. The integrals of $d\sigma$ over (I) and (II) are of course the same. The $\mathcal{O}(\alpha_s)$ contribution to the two-jet rate is therefore given by

$$\begin{aligned} \frac{\sigma_{2\text{-jet}}^{(\alpha_s)}}{\sigma_0} &= \frac{1}{\sigma_0} \left[2 \int_{(I)_a} d\sigma_g + 2 \int_{(I)_b} d\sigma_g + \int_{\text{virtual}} d\sigma_v \right] \\ &= \frac{4\alpha_s C_F}{\pi} \left[\int_0^{y\sqrt{s}} \frac{dk_0}{k_0} \int_0^1 \frac{d\cos\theta}{1-\cos^2\theta} + \int_{y\sqrt{s}}^{\sqrt{s/2}} \frac{dk_0}{k_0} \int_{1-(\frac{y\sqrt{s}}{k_0})}^1 \frac{d\cos\theta}{1-\cos^2\theta} \right. \\ &\quad \left. - \int_0^{y\sqrt{s}} \frac{dk_0}{k_0} \int_0^1 \frac{d\cos\theta}{1-\cos^2\theta} \right] \\ &= \frac{4\alpha_s C_F}{\pi} \left\{ - \int_{y\sqrt{s}}^{\sqrt{s/2}} \frac{dk_0}{k_0} \int_0^1 \frac{d\cos\theta}{1-\cos^2\theta} + \int_{y\sqrt{s}}^{\sqrt{s/2}} \frac{dk_0}{k_0} \int_{1-(\frac{y\sqrt{s}}{k_0})}^1 \frac{d\cos\theta}{1-\cos^2\theta} \right\} \end{aligned}$$

$$\begin{aligned}
&= \frac{4\alpha_s C_F}{\pi} \int_{y\sqrt{s}}^{\sqrt{s/2}} \frac{dk_0}{k_0} \int_0^{1-(\frac{y\sqrt{s}}{k_0})} \left(\frac{d \cos \theta}{1 - \cos^2 \theta} \right) \\
&= \frac{2\alpha_s C_F}{\pi} \int_{y\sqrt{s}}^{\sqrt{s/2}} \frac{dk_0}{k_0} \left[(-) \log \frac{k_0}{y\sqrt{s}} + (\text{finite for } y \rightarrow 0) \right] = -\frac{\alpha_s C_F}{\pi} \log^2 2y . \quad (\text{C.6})
\end{aligned}$$

Including the Born contribution, which always gives rise to two and only two jets, we finally have

$$\begin{aligned}
\sigma_{2\text{-jet}} &= \sigma_0 \left[1 - \frac{\alpha_s C_F}{\pi} \log^2 y + \dots \right] , \\
\sigma_{3\text{-jet}} &= \sigma_0 \frac{\alpha_s C_F}{\pi} \log^2 y + \dots .
\end{aligned}$$

If $y \rightarrow 0$, $\sigma_{3\text{-jet}}$ becomes larger than $\sigma_{2\text{-jet}}$. If y is sufficiently small, we can even get $\sigma_{2\text{-jet}} < 0$! This is a sign that higher-order corrections become important. In the soft-gluon limit, assuming that the emission of a second gluon will also factorize⁴, we can repeat the calculation at higher orders and obtain

$$\begin{aligned}
\sigma_{2\text{-jet}} &\simeq \sigma_0 \left[1 - \frac{\alpha_s C_F}{\pi} \log^2 y + \frac{1}{2!} \left(\frac{\alpha_s C_F}{\pi} \log^2 y \right)^2 + \dots \right] = \sigma_0 e^{-\frac{\alpha_s C_F}{\pi} \log^2 y} , \\
\sigma_{3\text{-jet}} &\sim \sigma_0 \frac{\alpha_s C_F}{\pi} \log^2 y e^{-\frac{\alpha_s C_F}{\pi} \log^2 y} , \\
&\vdots \\
\sigma_{(n+2)\text{-jet}} &\sim \sigma_0 \frac{1}{n!} \left(\frac{\alpha_s C_F}{\pi} \log^2 y \right)^n e^{-\frac{\alpha_s C_F}{\pi} \log^2 y} . \quad (\text{C.7})
\end{aligned}$$

It is immediate to recognize in this series a Poisson distribution, leading to an average number of jets given by

$$\langle n_{\text{jet}} \rangle \simeq 2 + \frac{\alpha_s C_F}{\pi} \log^2 y . \quad (\text{C.8})$$

The *smaller* the resolution parameter y , the *smaller* the mass of the jets, and the *larger* the importance of higher-order corrections. If we take the parameter M down to the scale of a few hundred MeV ($M \sim \Lambda_{\text{QCD}}$), each particle gets identified with an independent jet. We can therefore estimate the s -dependence of the average multiplicity of particles produced:

$$\langle n_{\text{part}} \rangle \sim \frac{C_F \alpha_s}{\pi} \log^2 \frac{s}{\Lambda^2} = \frac{C_F}{\pi} \frac{1}{b_0 \log \frac{s}{\Lambda^2}} \log^2 \frac{s}{\Lambda^2} \simeq \frac{C_F}{\pi b_0} \log \frac{s}{\Lambda^2} . \quad (\text{C.9})$$

The final-state particle multiplicity grows with $\log(s)$.

In practice, things are a bit more complicated than this. Once the first gluon is emitted, additional gluons can be emitted from it as well. Therefore the final-state multiplicity will be dominated by the emission of gluons from gluons. The analysis becomes more complicated (see e.g., Refs. [6] and [8] for the details), and the final result is

$$\langle n_{\text{part}}(s) \rangle \sim \exp \sqrt{\frac{2C_A}{\pi b} \log\left(\frac{s}{\Lambda^2}\right)} \quad (\text{C.10})$$

for the particle multiplicity, and

$$\langle n_{\text{jet}}(y) \rangle = 2 + 2 \frac{C_F}{C_A} \left(\cosh \sqrt{\frac{\alpha_s C_A}{2\pi} \log^2 \frac{1}{y}} - 1 \right) \sim \frac{C_F}{C_A} \exp \sqrt{\frac{\alpha_s C_A}{2\pi} \log^2 \frac{1}{y}}$$

⁴This is not true (see later on), but let us just accept it to see how things develop.

for the average jet multiplicity.

Other interesting quantities that can be calculated using the simple formulas we developed so far are the average jet mass and the thrust. To define the jet mass we just divide the final state into two hemispheres, separated by the plane orthogonal to the thrust axis. We now call jets the two sets of particles on either side of the plane. The $\langle m^2 \rangle$ of the jet is then given by

$$\langle m_{\text{jet}}^2 \rangle = \frac{1}{2\sigma_0} \left\{ \int_{\text{(I)}} (q+k)^2 d\sigma_g + \int_{\text{(II)}} (\bar{q}+k)^2 d\sigma_g \right\}. \quad (\text{C.11})$$

The virtual correction does not enter here, since the pure $q\bar{q}$ final state has jet masses equal to 0. The result of this simple computation leads to

$$\langle m_{\text{jet}}^2 \rangle = \frac{\alpha_s C_F}{\pi} s. \quad (\text{C.12})$$

Another interesting variable often used in experimental studies is the thrust T , defined by

$$T = \max_{\hat{T}} \sum_i |\vec{p}_i \cdot \hat{T}| / \sum_i |\vec{p}_i|$$

where \hat{T} is the thrust axis, defined so as to maximize T . For three-body final states, \hat{T} is the direction of the highest-energy parton, and T is proportional to twice its energy:

$$T = 2 \frac{\bar{q}_0}{\sqrt{s}} \equiv 1 - \frac{(q+k)^2}{s} = 1 - \frac{m_{\text{jet}}^2}{s}. \quad (\text{C.13})$$

As a result,

$$\langle 1 - T \rangle = \frac{\alpha_s C_F}{\pi}. \quad (\text{C.14})$$

At LEP, $\langle 1 - T \rangle \simeq \frac{0.120}{\pi} \times \frac{4}{3} \simeq 0.05$. The terms neglected in the soft-gluon approximation we used throughout can be calculated, and give some small correction to the above results. Corrections will likewise come from higher-order effects. State-of-the-art calculations exist which evaluate all these ‘shape variables’ (and more!) up to $\mathcal{O}(\alpha_s^2)$ accuracy, including a full next-to-leading-log accurate resummation of higher-order logarithms (such as the $\log 1/y$ terms we encountered in the discussion of jet rates, or terms of the form $\log^n(1-T)$ which appear at higher orders in the evaluation of the thrust distributions). These calculations allow a reliable estimate of several different observables directly proportional to α_s , and provide the theoretical input for the extraction of α_s from the LEP QCD data [8].

Note that non-perturbative corrections proportional to $\frac{\Lambda}{\sqrt{s}}$, with $\Lambda \sim 1$ GeV, can have a significant impact on the extraction of α_s . For example, a $\frac{\Lambda}{\sqrt{s}}$ correction to $\langle 1 - T \rangle$ would be a 20% effect:

$$\frac{\Lambda}{\sqrt{s}} \sim 0.01, \quad \langle 1 - T \rangle_{\text{PT}} \simeq 0.05.$$

Indeed one measures $\langle 1 - T \rangle_{\text{LEP}} = 0.068 \pm 0.003$, compared with the full perturbation theory QCD prediction of 0.055 (using $\alpha_s = 0.120$).

Acknowledgements

It is a pleasure to thank the organizers of this School for the successful efforts made to bring top-quality students together and to provide a great environment for physics discussions, and for a pleasant time as well.

Bibliography

Standard Textbooks

- [1] R.P. Feynman, *Photon–Hadron Interactions* (W.A. Benjamin, NY, 1972).
- [2] B.L. Ioffe, V.A. Khoze and L.N. Lipatov, *Hard Processes* (North Holland, 1984).
- [3] T. Muta, *Foundations of QCD* (World Scientific, 1987).
- [4] V. Barger and R.J.N. Phillips, *Collider Physics* (Addison Wesley, 1987).
- [5] R. Field, *Applications of Perturbative QCD* (Addison Wesley, 1989).
- [6] Yu.L. Dokshitzer, V.A. Khoze, A.H. Mueller and S.I. Troyan, *Basics of Perturbative QCD* (Editions Frontières, 1991).
- [7] M.E. Peskin and D.V. Schroeder, *An Introduction to Quantum Field Theory* (Addison-Wesley, 1995).
- [8] R.K. Ellis, W.J. Stirling and B.R. Webber, *QCD and Collider Physics* (Cambridge University Press, 1996).

Pedagogical Reviews

- [9] P. Nason, lectures delivered at the 1997 European School of High-Energy Physics, Menstrup, Denmark, CERN 98-03 .
- [10] Yu.L. Dokshitzer, lectures delivered at the 1995 European School of High-Energy Physics, Dubna, Russia, CERN 96-04.
- [11] M. Neubert, lectures delivered at the 1995 European School of High-Energy Physics, Dubna, Russia, CERN 96-04.

Review Articles

- [12] G. Altarelli, *Phys. Rep.* **81** (1982) 1.
- [13] A.H. Mueller, *Phys. Rev.* **73** (1981) 237.
- [14] Yu.L. Dokshitzer, D.I. Dyakonov and S.I. Trojan, *Phys. Rep.* **58** (1980) 270.
- [15] A. Bassetto, M. Ciafaloni and G. Marchesini, *Phys. Rep.* **100** (1983) 201.
- [16] M.L. Mangano and S.J. Parke, *Phys. Rep.* **200** (1991) 301.

Historical Reviews

- [17] D.J. Gross, hep-th/9809060.
- [18] G. 't Hooft, hep-th/9808154.